SKB

TECHNICAL REPORT 89-13

Spent fuel
Dissolution and oxidation
An evaluation of literature data

Bernd Grambow

Hanh-Meitner-Institut, Berlin

March 1989

SVENSK KÄRNBRÄNSLEHANTERING AB
SWEDISH NUCLEAR FUEL AND WASTE MANAGEMENT CO
BOX 5864 S-102 48 STOCKHOLM
TEL 08-665 28 00 TELEX 13108 SKB

SPENT FUEL, DISSOLUTION AND OXIDATION
An evaluation of literature data

Bernd Grambow

Hahn-Meitner-Institut, Berlin

March 1989

Dr. Bernd Grambow

Spent fuel
Dissolution and Oxidation

an evaluation of literature data

March 1989

Kuno Fischer Str. 7, D 1000 Berlin 19, Office in Hahn-Meitner-Institut Berlin GmbH, D 1000 Berlin 39, Glienicker Str. 100, ph. (004930)80092290

ABSTRACT

Data from studies of the low temperature air oxidation of spent fuel were retrieved in order to provide a basis for comparison between the mechanism of oxidation in air and corrosion in water. U_3O_7 is formed by diffusion of oxygen into the UO_2 lattice. A diffusion coefficient of oxygen in the fuel matrix was calculated for 25°C to be in the range of 10^{-23} to 10^{-25} m^2/s.

Reported rate data for the dissolution of UO_2, uraninite and spent fuel where compiled as a function of environmental variables. Within the scatter of data, resulting from uncertainties in the effective surface area, the initial rates of U release from spent fuel and from UO_2 appeared to be similar. The lowest rates (at 25°C $>10^{-4}$ $g/(m^2d)$) were observed under reducing conditions. Under oxidizing conditions the rates depend mainly on the nature and concentration of the oxidant and/or on carbonate. In contact with air, typical initial rates at room temperature were in the range between 0.001 and 0.1 $g/(m^2d)$.

A study of apparent U solubility under oxic conditions was performed and it was suggested that the controlling factor is the redox potential at the UO_2 surface rather than the E_h of the bulk solution. Electrochemical arguments were used to predict that at saturation, the surface potential will eventually reach a value given by the boundaries at either the U_3O_7/U_3O_8 or the U_3O_7/schoepite stability field, and a comparison with spent fuel leach data showed that the solution concentration of uranium is close to the calculated U solubility at the U_3O_7/U_3O_8 boundary. Nevertheless, a true thermodynamic equilibrium may never be achieved, because the U_3O_7 surface will remain unstable with respect to schoepite or other U(VI) phases if the concentration of oxidants in bulk solution is high enough.

The difference in the cumulative Sr and U release was calculated from data from Studsvik laboratory. The results reveal that the rate of Sr release decreases with the square root of time under U-saturated conditions. This time dependence may be rationalized either by grain boundary diffusion or by diffusion into the fuel matrix.

Hence, there seems to be a possibility of an agreement between the Sr release data, structural information and data for oxygen diffusion in UO_2. If this correlation is substantiated by comparison with other experimental data and by surface analytical techniques, the release of soluble radionuclides from spent fuel can in part be described as a transport process under moving boundary conditions.

SUMMARY AND CONCLUSIONS

Safe disposal of nuclear waste requires repository and waste package designs based on an understanding of long-term reaction scenarios in the event of waste form/ groundwater contact. The reaction behavior of spent nuclear fuel with groundwater is difficult to assess. At present only prelimnary models are available, which are not able to predict the long-term performance of the fuel. It is the aim of this study to evaluate and interpret literature data so that they can be used in the development of a release model for radionuclides from spent fuel.

If it could be ensured that reducing conditions will prevail at the fuel-groundwater interface, a model based on matrix solubility might be sufficient to describe the long-term release of fission products. If, however, due to radiation or other constraints oxidative conditions cannot be excluded, the situation is much less clear because UO_2 cannot approach thermodynamic equilibrium with an aqueous environment. Observations of the mechanism of oxidation of UO_2 in air and results from XPS surface analyses of UO_2 electrodes exposed to aqueous solutions show that the dissolving solid under oxic conditions is essentially U_3O_7.

Data from studies of the low temperature air oxidation of spent fuel were retrieved in order to provide a basis for comparison between the mechanism of oxidation in air and corrosion in water. U_3O_7 is formed by diffusion of oxygen into the UO_2 lattice. A diffusion coefficient of oxygen in the fuel matrix was calculated for 25°C to be in the range of 10^{-23} to 10^{-25} m^2/s. This is only slightly higher than the coefficient estimated for fission product release from the two billion year old natural Oklo reactor.

Reported rate data for the dissolution of UO_2, uraninite and spent fuel where compiled as a function of environmental variables. Within the scatter of data, resulting from uncertainties in the effective surface area, the initial rates of U release from spent fuel and from UO_2 appeared to be similar. The lowest rates (at 25°C $>10^{-4}$ $g/(m^2d)$) were observed under reducing conditions. Under oxidizing conditions the rates depend mainly on the nature and concentration of the oxidant and/or on carbonate. In contact with air, typical initial rates at room temperature were in the range between 0.001 and 0.1 $g/(m^2d)$.

The initial reaction rates may be of limited use for the evaluation of the spent fuel long-term behavior, since the solubility of uranium is considered to be a limiting factor for the release of soluble radionuclides from spent fuel. This is clear for reducing conditions. Under oxidizing conditions, the solubility-controlling uranium-containing phase is not UO_2 and a high thermodynamic driving force for UO_2 dissolution remains when secondary alteration products such as schoepite become saturated. Yet even under oxidizing conditions the experimental data show a decrease in the release rate of soluble radionuclides (i.e. ^{137}Cs, ^{90}Sr, ^{125}Sb) which approaches the rate of solubility limited U release with time.

A study of apparent U solubility under oxic conditions was performed and it was suggested that the controlling factor is the redox potential at the UO_2 surface rather than the Eh of the bulk solution. If the dissolving solid under oxic conditions is essentially U_3O_7, saturation effects with respect to this phase can be of importance for the overall reaction rate. Electrochemical arguments were used to predict that at saturation, the surface potential will eventually reach a value given by the boundaries at either the U_3O_7/U_3O_8 or the U_3O_7/schoepite stability field, and a comparison with spent fuel leach data showed that the solution concentration of uranium is close to the calculated U solubility at the U_3O_7/U_3O_8 boundary. Nevertheless, a true thermodynamic equilibrium may never be achieved, because the U_3O_7 surface will remain unstable with respect to schoepite or other U(VI) phases if the concentration of oxidants in bulk solution is high enough.

Determination of mass transfer rates for the conversion of U_3O_7 to higher oxide alteration products are very important as U_3O_7 will most likely retain soluble radionuclides whereas higher oxides may not.

In order to study the release of Sr under U saturated conditions, the difference in the cumulative Sr and U release was calculated from data from static, replenishment and sequential tests in deionized water and synthetic groundwater performed with high burnup BWR and PWR fuel at Studsvik laboratory [Forsyth, Werme 1986]. The results reveal that the rate of Sr release decreases with the square root of time under U-saturated conditions.

This time dependence may be rationalized either by grain boundary diffusion or by oxygen diffusion into the fuel matrix. An apparent diffusion coefficient was calculated from the ^{90}Sr data after conversion to an apparent depletion depth with an assumed effective surface area. Using the geometrical surface area a D value of $4*10^{-21}$ m^2/s is obtained. This is to be compared to a value D = 10^{-23} - 10^{-25} m2/s for the diffusion coefficient of oxygen. The diffusion coefficient calculated from the Sr release would comes closer to the oxygen diffusion coefficient when a fraction of grain boundaries is accessible to oxygen-containing water. This is just an effect of an increased surface area.

There is evidence that grain boundaries of spent fuel are at least partly accessible to water, as SEM micrographs of cross sections of leached spent fuel surfaces show open grain boundaries several grain diameters in length. Therefore, a significant fraction of fission products may be released from grain boundaries even if no segregation of these nuclides at the boundary occurs.

Hence, there seems to be a possibility of an agreement between the ^{90}Sr release data, structural information and data for oxygen diffusion in UO_2. If this correlation is substantiated by comparison with other experimental data and by surface analytical techniques, the release of soluble radionuclides from spent fuel can in part be described as a transport process under moving boundary conditions. Still, in the long run a steady state is expected, where the flow rate and solubility-controlled release rate of U equals the diffusion controlled transformation rate of the fuel matrix. Then the rate of U release will control the release of soluble fission products even under oxidizing conditions .

Table of Contents

I. INTRODUCTION

Direct disposal of spent nuclear fuel is reproted in many countries as a feasible strategy to protect the human environment from high level nuclear reactor waste. Barriers for radionuclide release to the environment are the geologic formation, the waste package, backfill and the fuel itself. In order to assess the ability of the fuel matrix to retain radionuclides, its reaction behavior with groundwater has been studied in many laboratories. The reaction scenario involves various sources of release: the fuel/sheet gap, grain boundaries, segregated fission product phases and the fuel matrix. Understanding of the dissolution behavior is further complicated by the fact that uranium has one of the most complex oxide systems in the periodic table. The solution and surface chemistry of UO_2 is quite complicated, a large variety of solid reaction products with different redox states can be formed with and without water contact and the radioactivity of the material makes experimental work very time consuming. Studies of the dissolution behavior of "non-radioactive" simulants (i.e. UO_2) must leave many questions open, such as the mass transfer rates under U-saturated conditions, the effect of grain boundaries and the interaction between groundwater and the various phases present in the fuel (fission products and actinides in solid solution, metallic and gaseous inclusions).

The ultimate goal of any study of the long-term performance of spent fuel as an individual barrier is a description of the rate of release of significant radionuclides as a function of environmental constraints at any time after final disposal. However, only in a few cases will the rates in a repository be the same as those obtained in the laboratory. The reason is that the water contact scenario and the sorption characteristics are different, and in the case of spent fuel the effect of radiation is not yet clear. In order to use laboratory data to predict behavior in a repository it is important to develop a model. At present, only prelimnary models are described in the literature.

It is the aim of this study to evaluate and to interpret literature data on UO_2, uraninite and spent fuel oxidation/dissolution in such a way that these data can provide a basis which would at some later time allow realistic modeling of the reaction path and the dissolution kinetics of the fuel matrix and radionuclide release in a repository. Currently the work is focussed on oxidizing conditions.

As oxidation of UO_2 may play an important role in the dissolution process, low- and high-temperature studies of fuel oxidation were briefly reviewed and a diffusion coefficient for oxygen in UO_2 was estimated for room temperature. For the dissolution of UO_2 and uraninite the effects of environmental variables on the initial reaction rates were considered following the description in the literature. An attempt is made to match contradicting views of various authors with the different experimental conditions studied. Reaction rate data were compiled for various conditions and were compared quantitatively with the initial rates observed in spent fuel leach tests. Corrosion data for spent fuel obtained at Studsvik laboratory were evaluated with respect to the mass transfer of radionuclides under U-saturated conditions. It is discussed whether saturation of U has any influence on the release rates of radionuclides, i.e. whether the solutions are saturated with respect to the dissolving solid or to an alteration product. An interesting result is that the mass transfer of soluble radionuclides under U-saturated conditions seems to follow a square root dependence on time. Correlation of fission product release with oxygen diffusion data was obtained.

II. EFFECT OF ENVIRONMENTAL VARIABLES ON THE DISSOLUTION RATES OF UO_2 AND NATURAL URANINITE - A STUDY OF LITERATURE DATA

The reaction kinetics of unirradiated or natural UO_2 with aqueous solutions have been studied for more than 30 years. Important research subjects have been acid or carbonate leaching of uranium from ores or conditions for nuclear reprocessing. Only a few studies (for example: Wang [1981], Ollila [1988]) address the question of mass transfer rates under conditions where uranium is saturated with respect to a secondary alteration product. These mass transfer rates are of course difficult to infer from studies of unirradiated UO_2 and may require the use of spent fuel or experimentally prepared solid solutions of UO_2 with soluble elements (see for example co-dissolution studies by Bruno and Sandino [1987]).

Important variables studied in the literature are pH, temperature, the nature and amount of oxidant, the concentration of carbonate and others. Yet no clear picture has emerged as to how the behavior of the various materials (UO_2, uraninite, spent fuel) can be compared. Moreover, quite contradictory effects of certain environmental variables are described. For example most authors [Thomas, Till 1984, Ollila 1988, Johnson 1988] believe that the degree of oxidation of the UO_2 surface has an important impact on the measured rates. In contrast, Grandstaff [1976] who performed one of the most elaborate studies of the rates of uraninite dissolution showed that at least for this already oxidized material, the degree of oxidation of the solid is only of minor importance in controlling reaction rates. Natural uraninite samples are in general much more oxidized than irradiated or unirradiated UO_2 pellets. A comparison of UO_2 dissolution data with corresponding uraninite data may help to evaluate the effect of surface oxidation.

Also the pH dependence of the reaction rate is not yet clear. Grandstaff [1976] reports for acid to neutral conditions a linear decrease of the rate with pH. In contrast, data from Thomas and Till [1982] show a decrease of reaction rate by only a factor of five between pH 1 and 4. Theories are reported that describe why there should [Grandstaff 1976] or should not be [Habashi, Thursten 1967] a pH dependence of the rate in the acid regime. In general the oxidative nature of the pH-controlling anion seems to be more important than the hydrogen ion concentration [Amell and Langmuir 1979].

For a quantitative representation of the observed effects of environmental variables, rate equations are described in the literature [Grandstaff 1976, Schortman, DeSea 1958, Pearson, Wadsworth 1958 and Habashi, Thursten 1967]. There is considerable disagreement in the rate laws if general applicability of the laws at various Eh, pH or carbonate concentrations is assumed. One may conclude that the equations are only applicable for the limited range of experimental conditions from which they were derived.

II. 1 Description of literature results

In the following a short critical account is given, author by author, of experimental conditions and major results of each of the studies considered.

Schortmann and DeSea [1958] studied the kinetics of dissolution of powdered uranium dioxide in carbonate/bicarbonate solutions (0 - 0.5 M) between 60 and 100°C. 99% of U was in the tetravalent state. The surface area of the sample was not reported but a linear dependence of the release of uranium on surface area was demonstrated by varying the powders' particle size and the ratio of solution volume to the amount of uranium dioxide present. The oxygen partial pressure was varied between 1 and 10 atm and the dissolution rate was found to be directly proportional to the square root of the oxygen partial pressure. The effect of temperature was described by an Arrhenius dependence with an activation energy of 13.4 kcal per mol of UO_2. The reaction rate was independent on the bicarbonate/carbonate ratio and dependent only on the total carbonate present. At "low" total carbonate concentrations of about 0.02 - 0.2 M the rate was found to be

proportional to the square of the carbonate content, whereas at higher carbonate concentrations a maximum rate is achieved. If one whishes to estimate reaction rates per surface area from geometric considerations of powder mesh sizes, the reaction rates observed by the authors would represent rates in the range of 10^4 g/(m^2d) equivalent to 1 mm/d. These rates are about 5 orders of magnitude higher than the rates obtained by Grandstaff (1976, see below), the effect being due to higher temperatures, oxygen partial pressure and carbonate content.

Pearson and Wadsworth [1958] studied the dissolution kinetics in carbonate solutions of sintered UO_2 disks of 99.94 % purity and 89 % of the theoretical density. The temperature was varied between 123 and 203°C and the oxygen partial pressure between 1 and 100 atm. The effect of carbonate was studied up to a concentration of 1.4 M. A maximum rate was observed at 1 M total carbonate and a carbonate/bicarbonate ratio of 3. At lower concentrations of total carbonate there was a pronounced dependence of the reaction rate on the stirring speed indicating rate control by transport of carbonate in the aqueous phase. This effect is not surprising as the maximum rates observed were extremely high i.e. in the range of $3*10^4$ g/(m^2d). With such high rates, transport processes can easily become the limiting factor. At very high carbonate concentration, the reaction rate decreases again. This was explained by the competition of sorption oxygen and H_2CO_3. The rate was found to be inversely proportional to the concentration of undissociated carbonic acid. The authors did not discuss the possible interference with their results of the formation of uranium carbonate precipitates.

Habashi and Thurston [1967] studied the dissolution kinetics of $UO_{2.04}$ in acid (H_2SO_4) and in carbonate media at a temperature of 100°C. The oxygen partial pressure was varied between 1 and 10 atm and the content of total carbonate between 0 and 0.5 M. Not very much data were presented, and due to a lack of experimental details it is not possible to derive quantitative information useful for comparing with other people's data sets. Still the described trends are very interesting. Their data indicate that in acid media the rate is proportional to the partial pressure of oxygen while in carbonate media the rate is proportional to the square root of the oxygen partial pressure. The latter finding agrees with that found by Pearson and Wadsworth [1958] and Shortmann and DeSea [1958]. In acid solutions (about pH 2) the rate was independent on pH, whereas at higher pH values the rate did not depend on oxygen but decreased linearly with the pH. The authors interpreted their results, similar to the dissolution of metals, as an electrochemical process. Like a metal, under oxidizing conditions UO_2 takes up electrons at one part of its surface (cathodic reaction: reduction of O_2) while it releases electrons at another part (anodic reaction: formation of uranyl ions from U(IV)). A low soluble U(VI) hydroxide is assumed to be formed at the surface. The cathodic reaction rate is assumed to be proportional to the oxygen partial pressure, whereas the rate of the anodic reaction is assumed to be proportional to the H+ concentration. At steady state anodic and cathodic reaction rates must be equal. This imposes constraints on the relative importance of the effect of pH and log (pO_2). At pH values lower than (4.7-log(pO_2)) there is no dependence of the reaction rate on pH and the surface hydroxide phase may readily dissolve. At higher pH values there is no dependence of the reaction rate on O_2 and a the surface hydroxide may be considered as insoluble. The value of 4.7 is given by the ratio between the rate constants for anodic and cathodic reaction. It is of course not possible to extrapolate this relationship to other temperatures as long as the respective rate constants are not known.

Nicol and Needs [1975, 1977] performed dissolution experiments with UO_{2+x} electrodes (x=0.01,0.03 and 0.14) (potentiostatic measurements, cyclic voltammograms and tests with a ring disc electrode) in perchlorate and carbonate solutions at a temperature of 25°C. To describe their results the authors derived an equation for the current under steady-state potentiostatic conditions which is consistent with a mechanism that involves (1) successive electron transfers to one or more surface intermediates, (2) the formation of U(VI) films and (3) the formation of U(VI) as the only soluble product. The latter condition may be questioned, as the dissolution of U(IV) surface species does not involve electron transfer, hence its dissolution cannot be excluded. The following limiting conditions are discussed. At low current density and/or acid conditions, surface film formation is slower than the dissolution reaction and two cases can be distinguished. (1) At pH < 2 and low anodic potentials the anodic current increases linearly with pH. (2) At higher potentials, the current is independent of pH up to pH 5. This is similar to the conclusions and data from the work of Habashi and Thurston (1967). At high current densities and high pH values (pH 9-13) the formation of surface films becomes important and a potential-independent current would be given by the pH dependence of the dissolution rate of that film. In carbonate solutions of low concentrations, the authors report a linear dependence of the rate of dissolution on the carbonate content. At high carbonate concentration and long anodization time UO_2CO_3 (rutherfordine) was formed on the electrode.

In a kinetic study of the dissolution of various natural uraninite samples (powders), **Grandstaff [1976]** studied the effect of pH (4-9), surface area, temperature (2 and 23°C), total carbonate (10^{-5}- 10^{-1} M), dissolved oxygen (log pO_2 = -0.7 to - 2.7), organic retardation (natural waters versus laboratory make-ups), and the effect of non-uranium cations in the uraninite. The surface area of the uraninite powder was measured by means of stereological analyses. The different uraninite samples contained between 10 and 50 wt% of uranium trioxide. Surprisingly, no dependence of reaction rate on oxidation state was observed. Amell and Langmuir [1979] pointed out that this may be a result of predominant dissolution of edges and other active sites. As has already been mentioned, at pH values below 6 the rate of few experimental data points was proportional to the concentration of hydronium ions. The author explained this behavior by reference to the surface dissociation equilibria. Grandstaff assumed that in principe this dependence would also hold true for higher pH values, but the rate does not decrease further with increasing pH because the effect of pH is compensated for by the rate-ac-

celerating effect of total carbonate. Similar to the findings of Shortman and DeSea [1958] Grandstaff found that the rate depends on total carbonate rather than on CO_3^{--} or HCO_3^- alone. As shown by the work of Nicol and Needs [1977] at low carbonate concentration the reaction rate increased linearly with the carbonate content, whereas a slower increase of reaction rate was observed at higher carbonate concentrations (0.05 M). The author observed a linear relationship between the dissolved oxygen content in solution and the reaction rate.

The dissolution rate of natural uraninite samples has also been studied by **Posey-Dowty et al. [1987].** The authors tried to simulate conditions of uranium roll-front ores using bicarbonate solutions in the narrow pH range of 7.0 to 8.2 at variable oxygen partial pressure. Far away from uranium saturation in solution, the rate was linearly dependent on the square root of the oxygen partial pressure. It was concluded that the rate limiting step is the cleavage of an oxygen-oxygen bond in adsorbed oxygen. On aproaching saturation the reaction rate decreased with a rate law which is first order with respect to uranium in solution. No attempt was made to identify the solubility controlling phase. The initial reaction rate was independent on the carbonate content of the solution, but the extent of dissolution was much higher in the presence of carbonate because the saturation concentration of U in solution was higher. The authors presumed that the effect of carbonate observed in other studies is an artifact which resulted from the effect of carbonate on the saturation concentration.

In a study of potential fluids for solution mining of sedimentary uranium deposits **Amell and Langmuir [1979]** studied the dissolution of $UO_{2.01}$ at temperatures between 15 and 45 C using Fe(III) and or sulfate as oxidants. Between pH 1 and 2.4 no pH and no clear Eh dependence of the reaction rate was observed. The data showed that the rate was almost linearly dependent on the total concentration of ferric iron in solution. With 1 mM Fe(III) at pH 2 the dissolution rate was about 500 times higher than in the absence of iron, confirming that some oxidant other than oxygen is needed for significant UO_2 dissolution to occur.

An electrochemical surface reaction model was used by **Hiskey [1979, 1980]** for interpretation of the dissolution behavior of UO_2. Leach data in carbonate or hydrogen peroxide media agreed well with a model, in which oxidation of UO_2 at anodic surface sites is coupled with reduction of an oxidant at cathodic sites. At anodic sites the formation of intermediate U(V) hydroxide or bicarbonate surface complexes occurs whereas the number of cathodic sites is given by the surface coverage of adsorbed O_2, which is related to the partial pressure of O_2 by Henry's law and by sorption equilibria. A mixed electrochemical potential is established at the UO_2 surface which is governed by the constraint that without external electromotive driving force anodic and cathodic currents must be equal. The mixed potential depends on the relative rates of anodic and cathodic reaction and this condition also imposes constraints on the reaction order with respect to the concentration of reactants such as oxygen or carbonate. For example, the author assumed that at a fixed (i.e. applied) surface potential, the rate of anodic oxidation of UO_2 would be linearly dependent on the solution concentration of bicarbonate. Without applied potential the reaction order with respect to carbonate is lower because the mixed potential will decrease with increasing carbonate content. Such a decrease was experimentally observed by Shoesmith et al. [1983] (see below). The decrease of the mixed potential implies that the cathodic reduction of oxygen is accelerated and the anodic dissolution rate of UO_2 is reduced. The result is that the dissolution reaction at a fixed pH is proportional to the square root of the bicarbonate concentration. In a similar way, the author showed that with a fixed bicarbonate content in solution, the reaction rate depends on the square root of the oxygen partial pressure. At high partial pressures of oxygen the reaction rate does not depend on oxygen because surface sites are occupied.

In deionized water, synthetic groundwater and in a sodium chloride rich brine, the dissolution of single crystal UO_2 surfaces and of spent fuel at oxygen pressures of about 6 atm was studied by **Wang [1981] and Wang and Katayama [1982]** using autoclave techniques at 75 and 150°C and electrochemical measurements at 25 and 75°C. Saturation was reached in all autoclave tests in less than 20 days. The reaction rate appears to be controlled by the availability of oxygen at the UO_2 surface. As long as an unlimited supply of oxygen exists the dissolution will continue even if the surface region of the solution has been supersaturated. Despite the fact that the solution concentration of UO_2^{2+} decreased with increasing temperature (due to the retrograde temperature dependence of the solubility of UO_3*2H_2O), the total dissolution of UO_2 was much higher at higher temperature, as evidenced by the high amounts of UO_3*2H_2O (deionized water) or sodium polyuranite (synthetic groundwater) formed. In contrast to deionized water in salt brine, only a small surface film was formed which seemed to passivate the surface from further oxidative dissolution. In all three solutions the open circuit potential varied between -60 to -20 mV and the respective anodic dissolution currents corresponded in all cases to about 1 g/(m^2d) at 25°C. At 75°C the rate was about three times higher. The electrochemical work confirmed the protective nature of the film formed in the brine solution and showed that under alkaline conditions a slightly protective UO_3*H_2O film can be formed from reaction with H_2O_2, despite the fact that this surface film is a surface precipitate which can easily be peeled off. Auger analyses of the surface composition profile (O and U data) have shown that in the surface beneath the precipitate (which has a O/U ratio of 4) the O/U ratio gradually decreased from 3 to 2. Wang [1980] explained this by the formation of a mixture of UO_3 hydrate and UO_{2+x} but it is important to state that such profiles are indicative for oxygen (and/or water) diffusion processes. The dissolution rates of spent fuel, determined from electrochemical measurements, were nearly an order of magnitude lower than on single crystal UO_2.. The open circuit potential was also higher. No clear passivating effect of brine solutions was observed.

A detailed study of the surface reaction products of UO_2 has been performed by **McIntyre et al. [1981], Shoesmith et al. [1983, 1984, 1985] and Sunder et al. [1981, 1983]** using electrochemical (potentiostatic and cyclic voltammetric) techniques and XPS. An electrode

was produced from a polycrystalline unirradiated fuel pellet. The U(IV)/U(VI) ratio at the electrode surface after the experiments was deduced from the shape of the U(4f7/2) peak in the photoelectron spectra. The sequence of reaction products is interpreted as UO_{2+x}, U_3O_7, U_2O_5, U_3O_8 and UO_3*xH_2O. As evidenced by comparing anodic (dissolution + oxide film formation) and cathodic (reduction of oxide films) charge transfers on UO_2 electrodes, dissolution can occur when the oxygen content of the surface film is higher than given by the stoichiometry of U_3O_7. Dissolution occurs via a UO_2^{2+} surface intermediate, which may either be still part of the oxidized surface layer or may be a sorbed species. Depending of the relative rates of dissolution and film formation, the composition of the outermost surface plane may be that of U_3O_7, U_2O_5 or U_3O_8. The authors measured an open circuit potential ("corrosion potential","mixed potential") which was about 50 to 100 mV (slightly higher than the values measured on single crystals by Wang [1980]) and between pH 3 and 9 almost independent of pH. At this potential anodic and cathodic currents are equal, which means that also in non-electrochemical dissolution studies surface potentials of similar magnitude will be established provided that UO_2 dissolves even if the bulk solution Eh is much higher. At high potentials $UO3*xH_2O$ formed as a precipitate in the absence of stirring. Results [Johnson et al. 1981] from long-term experiments (60 days) performed at constant current suggest that this precipitate is non-protective. In carbonate solutions a variable reaction order with respect to carbonate was found. At low potentials (100 mV) and low carbonate concentrations the reaction was independent on carbonate. At higher carbonate concentrations the reaction was first order with respect to carbonate. At high potentials (200 mV) and high carbonate concentrations (0.001M) the rate depends on the square root of the carbonate concentration. Due to complexation in solution ($UO_2(CO_3)_3^{4-}$) UO_3*xH_2O did not form, and at carbonate concentrations higher than 1 mM oxides higher than U_3O_7 were not formed. Instead a UO_2CO_3 surface phase was observed.

The dependence of the dissolution rate of UO_2 fuel pellets on pH, the carbonate concentration and pO_2 has been studied by **Thomas and Till [1984]**. The results were widely quoted and plots for the pH dependence of the reaction rate at 40°C were reproduced by Johnson et al. [1988], Ollila [1986] and Reimus et al. [1988]. From pH 1 to 4 the rate decreased from 0.005 g/(m^2d) at pH 1 by only a factor of 5. The lowest rate was measured at pH 8 (10^{-4} g/(m^2d)). Although the observed effects are quite interesting, the data are difficult to interpret quantitatively because of inconsistency in the reported behavior. Units at figures sometimes do match neither the figure captions nor their reference in the text (Fig. 1 and 2 ct.). The reported dissolution rate at 40°C in deionized water was 0.003 g/m^2d when the data were plotted in the frame of a temperature dependence study and the rate reported for neutral pH in the frame of the pH dependence study was more than 30 times lower for the same temperature. A possible explanation is that some error in the unit conversions occurred, because in the same paper 3 different units for rates were used (mg/(m^2d), g/(cm^2d), kg/(m^2d)).

The dissolution of unirradiated UO_2 as a function of environmental variables was studied by **Ollila [1985, 1986, 1988]**. Leach solutions were deionized water and various synthetic groundwater compositions under oxic and anoxic conditions. Dissolution rates were derived [Ollila 1985] from tests with periodical replacement of the leachant following the ISO standard method 1982 (1, 3, 7 day, then weekly and after 6 weeks monthly), but since the solution concentrations of U seemed to be independent of the solution residence time, it can be concluded that saturation has been achieved from the first day and the measured rates are therefore controlled by the quotient of saturation concentration and residence time. An item of information important for the kinetics of the dissolution process is that the rate was high enough to saturate the solution within one day. Using geometric sample surface area and solution volume, the initial rate under oxidizing conditions at 25°C can be calculated to be higher than about 0.02 g/(m^2d). The author showed that the mass transfer under U-saturated conditions can be strongly influenced by the formation of precipitates, coprecipitates or adsorbed materials.

The kinetics of dissolution of UO_2 under reducing conditions was first studied by **Bruno et al. [1987, 1988]** under a constant H_2(g) atmosphere using a Pd catalyst. In static and dynamic experiments the measured solution concentrations were higher than the solubility limit of UO_2 indicating that the rate of dissolution of an oxidized surface was studied. In dynamic corrosion tests at high flow rates the solution concentrations decreased after a maximum value had been reached, approaching UO_2 solubility in the long-term. This decrease was interpreted as a dissolution of the initially oxidized surface material. Although the closeness of the data to saturation may not allow an unambiguous interpretation of the data in terms of absolute forward reaction rates, the experimental results contain important information on the kinetics of dissolution under reducing conditions, because for the first time it was shown that oxidation of the UO_2 is not a necessary step for dissolution. The reaction rates are high enough to saturate fast flowing solutions. If dissolution under oxidizing conditions occurs with oxidation as the rate-limiting step, this only means that oxidation is faster than dissolution of U(IV). A pH-dependent lower limit for the reaction rate under reducing conditions can be obtained from the surface area of the samples and the pH dependence of the observed final solution concentration.

II. 2 Summary of the current understanding of the effect of environmental parameters on the dissolution kinetics of UO_2 and uraninite

The majority of authors seems to agree that the dissolution reaction is a surface reaction, which means that under diluted conditions the

rate is constant with time and proportional to surface area. However, in explaining the effect of environmental variables on the reaction rate, two lines of interpretation of UO_2 dissolution data can be distinguished in the literature: an electrochemical and a chemical explanation. The difference is that in an electrochemical dissolution model the reactions at two reactive sites (anodic oxidation, cathodic reduction) are coupled by charge conductance in the low-resistance dissolving material, whereas in a chemical model oxidation of UO_2 and reduction of the oxidant occur in the same reaction (possibly through different reaction steps). The effects observed and the interpretations offered can be summarized as follows:

Effect of partial pressure of oxygen and effect of other oxidative agents:

- under strongly reducing conditions the rate is low but higher than 10^{-4} g/(m2d)
- in espite of the different models used for interpretation, there seems to be general agreement that in acid media the rate depends linearly on the partial pressure of oxygen (between 0.01 and 100 atm O_2), since the oxidation of UO_2 is rate limiting.
- at low pH the rate is also proportional to the concentration of other oxidative agents (Fe(III), H_2O_2) and the rates can be much higher than in the presence of oxygen. What is important is not the system's Eh, but the nature of the agent.
- in carbonate media at high oxygen partial pressures, the dissolution rate depends on the square root of the oxygen potential, due to sorption and either decomposition of oxygen molecules at the surface or coupling of anodic and cathodic reactions. At low oxygen partial pressures (0.2 atm O_2), the rate may depend linearly on the oxygen content of the solution [Grandstaff 1976] when the adsorption rate is limiting.

Effect of carbonate under oxic conditions

- the effect of carbonate on the initial reaction rate of UO_2 is not very well understood. If one follows the interesting work of Posey-Dowty et al. [1987], there is no effect of carbonate on the forward rate of reaction and only the saturation concentration is depending on carbonate.
- most proposed mechanisms for the effect of carbonate describe only a small range of experimental conditions. The effect of saturation is usually not considered. Extrapolation to other conditions is difficult. For example, none of the reported rate laws can be used to extrapolate rates from a carbonate-containing system to a carbonate free environment.
- at low carbonate content (.001 M) the rate of UO_2 dissolution is proportional to total carbonate, when the rate of sorption of carbonate at the surface is the slow step in the reaction mechanism [Grandstaff 1976].
- at higher concentrations (.5 M) of carbonate the rate depends on the square root of the total carbonate concentration, because the rates are becoming so large that solution transport of carbonate to the surface [Pearson and Wadsworth 1958] or dissolution of an initially formed UO_2CO_3 film [Shoesmith et al. 1983] may control the overall rate .
- at even higher carbonate concentration (1M at 100°C) the dissolution rate reaches a maximum value. Thereafter, the reaction rate decreases either because there is a competition for surface sites between oxygen and carbonate [Pearson and Wadsworth 1958] or because the formation of surface films (UO_2CO_3) limits the rate [Nicol and Needs, 1977].

Effect of surface films

- films of UO_3*xH_2O seem in some cases to be non-protective, whereas in other case a passivating effect was observed
- sodium uranate films also seem to have no effect on the rate
- films formed by interaction with NaCl brines or high concentrations of H_2O_2 seem to passivate the UO_2 surface in some cases
- $UO_2CO_3(c)$ formation is sometimes associated with a decrease in the anodic current in electrochemical dissolution tests

Effect of pH

- at pH values between 0 and 4 under oxidizing conditions only a slight dependence of the reaction rate on pH was observed. This was attributed to the electrochemical nature of the UO_2 surface reaction
- between pH 4 and 6 a linear dependence of the reaction rate on pH was observed [Grandstaff 1976]. This would still be in agreement with the electrochemical mechanism [Habashi and Thursten 1967].
- at alkaline pH values, the reaction rate law depends both on the hydroxyl ion concentration and on carbonate, the rate being inversely proportional to the square root [Hiskey 1980] or the concentration [Grandstaff 1976] of hydroxyl ions.

II. 3 Quantitative comparison of reaction rate data

In this section an attempt is made to compare various rate data quantitatively. Included are rate data calculated from the initial U release measured in a spent fuel dissolution test. A more detailed examination of spent fuel data is presented in chapter IV.

In order to permit quantitative comparison of rate data from different research groups, the published rate values were normalized to surface area and expressed in units of $g/(m^2d)$. Only data from those authors who report pertinent experimental details to allow unit conversion were included. The data used are summarized in Table 1. The duration of the experiments is noted in the table. An explanation of how surface areas are calculated is given below. As far as possible, only data where U saturation could be excluded were used (rate data not derived from the quotient of saturation concentration and experimental time). Exceptions were made from the data from experiments performed under reducing conditions and for the initial release data from spent fuel tests.In the latter case, only data where there was some indication that the solution concentration of U increases with time were used (for example in low burnup fuel "SFLB" in Tab.1) but the possibility cannot be excluded that solubility limits are already attained. In this sense the data for the experiments performed under reducing conditions and the spent fuel data give a lower limit of the actual rate.

Methods and problems in estimation of sample surfaces areas

An important unknown is often the surface area. Assumptions had to be made which limit the accuracy of the comparison. No comparison would be possible if those assumptions were not made because, the dissolution of UO_2 in diluted solutions is proportional to surface area (see above). The methods used for estimation of surface area are described below. For estimation of the surface area of powdered samples, three methods were used:

- as far as data from stereological analyses were available, these were used
- as far as only BET surface measurements were available, these data were used for powdered samples
- for other experiments with powders, the rate was calculated from the mesh size of

No	Author	Material	Experiment	time [d]	T [C]	pH	pCO2	pO2	Rate	Sat	SA_met
1	Bruno	UO2	stat/ox	5	25	3	-3.5	-0.68	0.04	N	BET
2	Bruno	UO2	fl/red		25	4	-15	-15	0.0032	?	BET
3	Bruno	UO2	fl/red		25	4.5	-15	-15	0.0013	?	BET
4	Bruno	UO2	fl/red		25	6	-15	-15	0.0002	?	BET
5	Bruno	UO2	fl/red		25	6.7	-15	-15	0.00032	?	BET
6	Bruno	UO2	fl/red		25	6.8	-15	-15	0.00008	?	BET
7	Bruno	UO2	fl/red		25	7.8	-15	-15	0.000064	?	BET
8	Bruno	UO2	fl/red		25	8.1	-15	-15	0.00006	?	BET
9	Bruno	UO2	fl/red		25	9.8	-15	-15	0.0002	?	BET
10	Bruno	UO2	fl/red		25	11	-15	-15	0.00013	?	BET
11	Bruno	UO2	stat/red	0.5	25	3	-15	-15	0.00025	?	BET
12	Bruno	UO2	stat/red	0.5	25	5	-15	-15	0.0011	?	BET
13	Bruno	UO2	stat/red	0.1	25	12	-15	-15	0.0025	?	BET
14	Brodda	HTR	stat/ox *	100	20	5	-3.5	-0.68	0.085	N	geom
15	Brodda	HTR	stat/ox *	250	20	5	-3.5	1.48	1.8	N	geom
16	Grandsta	Uraninit	stat/ox	1	23	6.2	-3.5	-0.68	0.2	N	stereo
17	Grandsta	Uraninit	stat/red	4	23	5.6	-3.5	-1.68	0.02	N	stereo
18	Grandsta	Uraninit	stat/red	7	23	5.6	-3.5	-2.68	0.002	N	stereo
19	Grandsta	Uraninit	stat/ox	3	23	6	-3.5	-0.68	0.042	N	stereo
20	Grandsta	Uraninit	stat/red	4	23	5.6	-3.5	-1.68	0.0042	N	stereo
21	Grandsta	Uraninit	stat/red	7	23	5.6	-3.5	-2.68	0.0006	N	stereo
22	Grandsta	Uraninit	stat/ox	1	23	4.9	-3.5	-0.68	0.19	N	stereo
23	Grandsta	Uraninit	stat/ox	1	23	3.9	-3.5	-0.68	3	N	stereo
24	Grandsta	Uraninit	stat/ox	0.5	23	7	-3.5	-0.68	0.01	N	stereo
25	Grandsta	Uraninit	stat/ox		23	8.5	-3.5	-0.68	0.01	N	stereo
26	Fors/Wer	SFLB	seq/ox	55	25	8.1	-3.5	-0.68	0.02	N	geom
27	Fors/Wer	SFLB	seq/red	55	25	8.1	-15	-15	0.00015	N	geom
28	Fors/Wer	SFHBWR	repl/ox	47	25	8.2	-3.5	-0.68	0.01	?	geom
29	Fors/Wer	SFHBWR	seq/ox	20	25	2	-3.5	-0.68	0.16	N	geom
30	Fors/Wer	SFHBWR	seq/ox	20	25	3.2	-3.5	-0.68	0.07	N	geom
31	Fors/Wer	SFHBWR	seq/ox	20	25	3.4	-3.5	-0.68	0.12	N	geom
32	Fors/Wer	SFHBWR	seq/ox	20	25	4	-3.5	-0.68	0.054	N	geom
33	Fors/Wer	SFHBWR	seq/ox	20	25	4.1	-3.5	-0.68	0.026	N	geom
34	Fors/Wer	SFHBWR	seq/ox	20	25	5.5	-3.5	-0.68	0.0025	?	geom
35	Grandsta	Uraninit	stat/ox	1	23	8.3	-3.5	-0.68	0.01	N	stereo
36	Grandsta	Uraninit	stat/ox	1	23	8.3	-3.2	-0.68	0.02	N	stereo
37	Grandsta	Uraninit	stat/ox	1	23	8.3	-3	-0.68	0.038	N	stereo
38	Grandsta	Uraninit	stat/ox	1	23	8.3	-2.6	-0.68	0.08	N	stereo
39	Grandsta	Uraninit	stat/ox	0.5	23	8.3	-2.5	-0.68	0.11	N	stereo
40	Grandsta	Uraninit	stat/ox	0.5	23	8.3	-2.2	-0.68	0.22	N	stereo
41	Grandsta	Uraninit	stat/ox	0.5	23	8.3	-2	-0.68	0.35	N	stereo
42	Grandsta	Uraninit	stat/ox	0.25	23	8.3	-1.5	-0.68	0.64	N	stereo
43	Grandsta	Uraninit	stat/ox	0.25	23	8.3	-1.2	-0.68	0.72	N	stereo
44	Grandsta	Uraninit	stat/red	1	23	4.7	-1.5	-2.68	0.45	N	stereo
45	Grandsta	Uraninit	stat/ox	1	23	5.2	-2.4	-1.68	0.13	N	stereo
46	Wang **	UO2	Elek/ox		25	9.3	-3.1	0.7	1	N	geom
47	Wang **	UO2	Elek/ox		25	6.6	-3.5	0.7	1	N	geom
48	Schortma	UO2	stat/ox		25	10	-2.8	0.5	200	N	mesh
49	Preez	UO2	stat/ox	1	25	10	-2.8	-0.68	180	N	mesh
50	Hiskey	UO2	stat/ox		25	9.8	-2.4	0	0.96	N	disk
51	Hiskey	UO2	stat/ox		25	9.8	-2.4	0.43	1.57	N	disk
52	Hiskey	UO2	stat/ox		25	9.8	-2.4	0.87	2.6	N	disk
53	Hiskey	UO2	stat/ox		25	9.8	-2.4	1.16	3.3	N	disk
54	Fors/Wer	SFHBWR	bent/ox	27	25	8.7	-3.5	-0.68	0.00055	?	geom
55	Fors/Wer	SFHBWR	bent/ox	266	25	8.7	-3.5	-0.68	0.00035	?	geom
57	Fors/Wer	SFHBWR	seq/ox	20	25	8.2	-3.1	-0.68	0.0018	?	geom
58	Ollila	UO2	stat/ox	50	25	5.7	-3.5	-0.68	0.0006	?	geom
59	Ollila	UO2	stat/ox	50	25	8.2	-3.5	-0.68	0.0003	?	geom
60	Ollila	UO2	stat/ox	50	25	8.3	-3.2	-0.68	0.002	?	geom
61	Ollila	UO2	stat/ox	50	25	8.3	-2.5	-0.68	0.02	?	geom
62	Bruno	UO2	stat/red	0.1	25	6.9	-2	-15		?	BET
63	Bruno	UO2	stat/red	0.1	25	6.4	-1.3	-15		?	BET
64	Bruno	UO2	stat/red	0.1	25	6.9	-1.3	-15		?	BET
65	Bruno	UO2	stat/red	0.1	25	8	-1.3	-15		?	BET

Table 1: Compilation of apparent initial dissolution rates for UO_2, spent fuel and uraninite. Units: time [d], rate [g/(m^2d)], temp [°C], notations: author Brodda et al. [1987], Bruno et al. [1987,1988], Forsyth and Werme [1986], Grandstaff [1976], Hiskey [1980], du Preez et al. [1980], Posey-Dowty et al. [1987], Schortman and de Sea [1958], Wang [1981]. materials HTR = high temperature reactor fuel, SFHB = high burnup BWR fuel, SFLB = low burnup fuel, UO_2 = UO_{2+x} with $0<x<0.1$, uraninite M and NC = naturally occuring uraninite with U(IV)/U(VI) = 6.1 (M) and = 0.49. experiment Elek/ox = electrochemical study, fl/red = flow test H2/Pd condit., repl/ox = replenishment test oxidizing, seq/ox = sequential test oxidizing, stat/ox and stat/oxc = static test oxidizing, stat/red = static tests reducing; pCO_2, pO_2 = logarithmic values, log pO_2 and pCO_2 data value of -15 arbitrarily used for H2/Pd test. * Test performed in high concentrated MgCl2 rich brines with a single 500 µm sphere. ** There are other data with lower release rates, but saturation is likely. SAT=saturation state of the solution: N = no saturation. SA_met: method for estimation of surface area. geom.= SA estimated by average particle size, stereo= SA from stereological evaluation, disk= geometrical SA of a disk sample.

the sieves used in preparation of the powder fractions ("mesh" in Tab. 1)

- The magnitude of the error associated with either BET or grain size measurement of powder surface area was not known, but an example may serve to illustrate the uncertainty: The BET specific surface area of the samples used in the work of Bruno et al. [1988] was 0.2 m2/g. This would correspond to a calculated mean particle size of between 1 and 3 μm. The reported particle size of the material used was 50 μm, corresponding to a ten times smaller specific surface area. It could well be that fines contribute to the high BET surface area, but it is also possible that the BET measurements do not give accurate absolute surface area values.
- In the case of larger samples (fuel pellets, single crystal, spent fuel fragments) the geometrical surface area was used ("geom" in Tab.1).

Certain comments concerning the surface area of spent fuel are offered here which may also be of relevance in the evaluation of spent fuel data given below.

- in cases where the geometrical surface area is estimated from fuel segment samples errors can be introduced by statistical variations in the shape and size of fragments. The error in surface area and hence its contribution to the error is the derived rates would not be higher than a factor of two.
- fines were neglected, which could mean that the effective surface area is higher than the geometric surface area
- if water can penetrate the open grain boundary porosity of used fuel then the effective surface area may be much higher than the geometrical. A maximum value for the surface area would be that of separated grains. This is about a factor of 200 higher than the geometrical surface area.
- the porosity of as-fabricated UO_2 pellets is a design criteria and may vary between 1 and 5%. Assuming that this would mean open porosity a maximum increase in surface area of only 14% was calculated (spherical model pores). Therefore, this effect is of minor importance.

Graphic comparison of the literature data

Rate data obtained at 25°C are compared in this section. To give a general overview of all data considered in Fig 1a-c, the rates are plotted as a function of pH. These three figures are essentially one: each plot gives different information on the same data, and a proper understanding of the plots requires comparison between them. Figure (a) shows the authors and the material studied, Figure (b) describes the experiment and Figure (c) gives log pO_2. The rate obtained from the work of du Preez et al. [1980] may be too high, as the geometric surface area was estimated from the mesh size of the sieves used to prepare the powder fractions, and fines were not taken into account. Data from Thomas and Till [1984] were not considered, due to the difficulties in their quantitative interpretation (see above).

As can be seen, the reaction rates of UO_2 may vary by as much as 6 orders of magnitude. Comparison of oxidizing and reducing tests shows that the effect of oxygen partial pressure seems to be more pronounced at high than at low pH. However, as the data under reducing conditions represent lower limiting values only, the observed effect may be caused by low U solubility under reducing conditions. It may be noted that if the reported units in the paper by Thomas and Till [1984] are correct, their data (rates between 0.001 and 0.0001 g/(m^2d)) for pH values between 3 and 12 under oxidizing conditions at 40°C are much lower than the rates reported for oxidizing conditions by all other authors and would be very close to the rates under reducing conditions (data of Bruno et al. [1988]). This is another reason for not using their data in this comparison.

The data from tests performed under air saturated conditions (log pCO_2 = -3.52, log

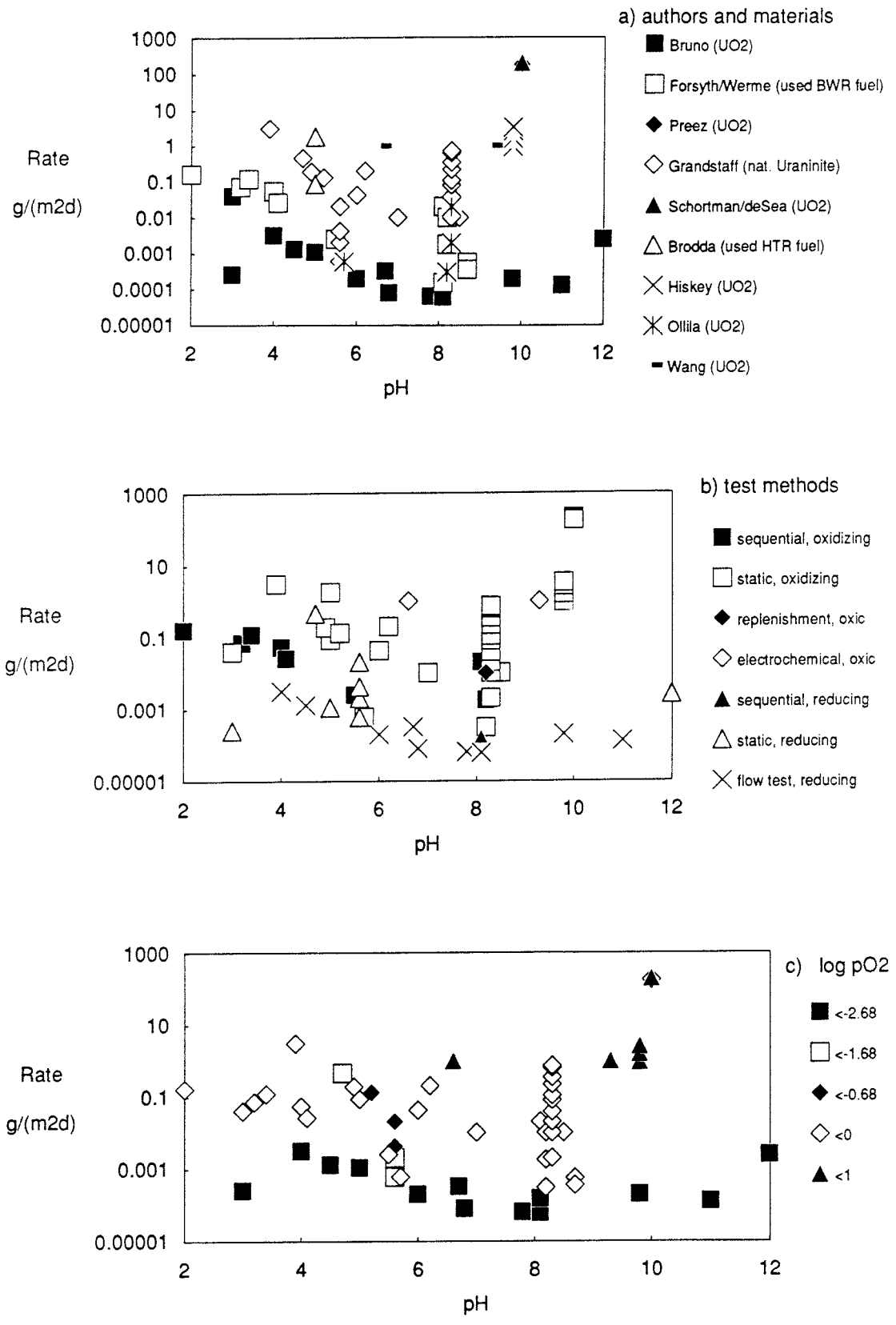

Figure 1: Comparison of initial dissolution rate data [g/(m^{2}d)] of used and unused UO_2 fuel and of natural uraninite. a) references and materials studied: Brodda et al. [1987], Bruno et al. [1987,1988], Forsyth and Werme [1986], Grandstaff [1976], Hiskey [1980], du Preez et al. [1980], Schortman and de Sea [1958], Wang [1981], Ollila [1988]. b) used tests, c) log pO_2 data

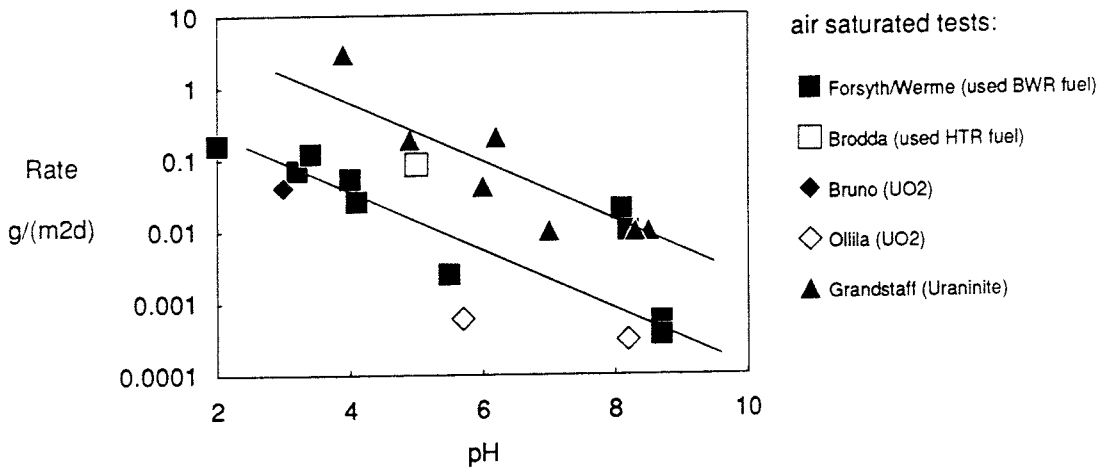

Figure 2: Initial dissolution rates [g/m^{2}d] of UO_2, spent fuel and uraninite under air saturated conditions (log pCO_2 = -3.52, log pO_2 = -0.68). Notations as in Fig. 1

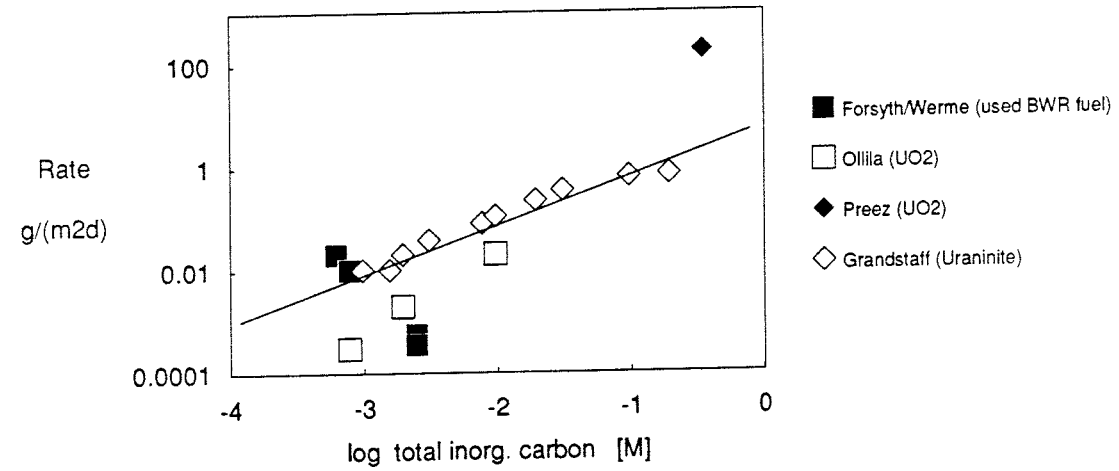

Figure 3: Dissolution rates [g/(m^{2}d)] as a function of total carbonate concentration [mol/l]. Only data with pH higher than 6 are plotted. Key to Symbols as in Figures 1

pO_2 = -0.68) are given as a function of pH in Figure 2. It is important to note that unirradiated UO_2 and high-burnup BWR fuel ("SFHBR") react at about the same rate. An interesting result is that the majority of rate values obtained for either unirradiated or used UO_2 fuel are 1 to 2 orders of magnitude lower than the rates for natural uraninite. This indicates that the oxidation state of the dissolving material is an important factor. Yet the rate law seems to be the same for both classes of material. The scatter in the data is too high to determine a reaction order with respect to the pH and the two plotted curves with a slope of -0.5 serve only as a guide for the eyes. Yet it appears to be clear that the reaction order is much less the value of -1 that was proposed by Grandstaff [1976] from very few data points. The data allow interpretation either by a square root dependence over the whole pH range considered, or according to Habashi and Thurston [1967] in terms of a pH-independent rate at low pH values and a pH-dependent rate at high pH.

The rates as a function of total carbonate under oxidizing conditions are given in Fig. 3. Due to a lack of reported experimental details it was not possible to compare the data of the various authors who studied the dissolution behavior of UO_2 in a carbonate environment. Again the value of du Preez [1980] seems to be too high. The plot show a clear increase in the rates with increasing total carbonate content of the solutions as long as the reaction rate is higher than 0.001 g/(m^2d). The linear dependence on total carbonate seems to be most reasonable. This must, however, be treated with caution as the plot is dominated by the data of Grandstaff [1976] (natural uraninite). Due to a lack of comparable data it is not possible to evaluate the results in terms of the above-described dependence of the reaction mechanism on total carbonate.

III. OXIDATION STUDIES OF UO_2 AND SPENT FUEL- AN ATTEMPT TO DERIVE A DIFFUSION COEFFICIENT FOR OXYGEN AT 25°C FROM LITERATURE DATA

Why study the kinetics of UO_2 oxidation in a paper on spent fuel dissolution? It has long been recognized that oxidation of UO_2 under water and in air follow different mechanisms [Aronson 1958]. The activation energy for a weight gain in water (87-200°C) is only about 5-10 kcal/mol, while in air it is about 26 kcal/mol. The final reaction product in contact with water may be in stoichiometry $UO_3*0.8H_2O$ [Aronson 1961], whereas air oxidation first produces β-U_3O_7 (possibly preceded by the formation of UO_{2+x}, and eventually U_3O_8. However, recent results of XPS surface analysis have shown (see above, [Sunder et al. 1981]) that the corrosion of UO_2 in contact with oxygen-containing water also may proceed via the formation of UO_{2+x} and U_3O_7. Therefore, the initial reaction steps of UO_2 in air and in water may be quite similar, and it is useful to investigate whether the results of low-temperature oxidation studies of UO_2 might contribute to an understanding of the corrosion mechanism for UO_2 in oxidizing aqueous solutions.

III.1 Mechanistic considerations

The overall oxidation mechanisms for spent fuel and UO_2 are quite different. The rate of oxidation is much higher in irradiated fuel than in nonirradiated materials [Hastings et al. 1985]. In the case of oxidation of spent fuel, the segregation of fission products, and particularly the formation of closely packed fission gas bubbles along grain boundaries, creates easy pathways for penetration of oxygen and internal oxidation [Woodley et al. 1988]. The overall rate of oxidation of spent fuel is therefore given by a combination of matrix and grain boundary oxidation [Einziger and Woodley 1985]. Initially the oxidation rate is low because only the geometric surface area is available for oxidation. With time the reaction rate increases considerably to a maximum value which is achieved when all grain boundaries are oxidized, i.e. the total grain surface area is accessible to the oxidation process [Einziger and Woodley 1985, 1987]. During the course of the oxidation process, the degree of attack may be quite inhomogeneous. There are sometimes high-density regions in the fuel where grain boundary oxidation is slow, and a situation could arrise where certain grains at some places in the fuel are completely oxidized, while grain boundaries at other places are not yet oxidized at all [Woodley et al. 1988].

The degree of matrix oxidation depends on temperature, time, and surface area, and below 0.007 atm O_2 on the partial pressure of oxygen as well. Even at temperatures as low as 25°C the reaction may proceed to the stage of UO_3*xH_2O [Hoekstra et al. 1961, Wadsten 1977] provided that the specific surface area is high enough, as it is the case with "active" UO_2 which has a specific surface area of about 30 m2/g. However, when the oxidation of fuel pellets below 160°C is studied, the formation of β-U_3O_7 appears to be the final product formed within in reasonable time intervals [Hoekstra et al. 1961]. Above 200°C γ-U_3O_7 and then U_3O_8 will be formed [Kuz'micheva et al. 1971]. The formation of U_4O_9 was suggested as an intermediate step at low oxidation rates prior to the formation of tetragonal U_3O_7 [Anderson et al. 1955]. However, a phase diagram given by Hoekstra et al. [1961] indicates that U_4O_9 may not form below 150°C, and in the oxidation studies of Kuz'micheva et al. [1971] the formation of U_4O_9 was never observed at low temperatures. In contrast, recent observations indicate that at 140 to 225°C, U_4O_9 is the major initial reaction product, at least in grain boundaries [Woodley et al. 1988].

The first oxidation step is the adsorption of an oxygen monolayer [Anderson 1953]. The

adsorption is fast and proceeds with an activation energy of 12.8 kcal/mol. The rate is linearly dependent on the partial pressure of oxygen [Smith 1960]. The further oxidation of UO_2 to β-U_3O_7 involves the diffusion of oxygen into the UO_2 lattice, with some distortion of the structure but without major structural reorganization of the parent fluorite lattice [Aronson et al. 1957, Taylor et al. 1980]. A superlattice will be formed, which has been explained in terms of long-range ordering of oxygen cluster chains [Allen and Tempest 1982]. The cluster chains represent a one-dimensional "path" of different chemical and physical properties within the conventional fluorite structure. Allen and Tempest [1982] predicted an inhomogeneous diffusion path with hindered diffusion along the cluster chains and easier diffusion between the chains.

Many authors suggested that oxygen diffusion controls the rate of UO_2 oxidation, either through a surface layer of U_3O_7 or within the UO_2 lattice, by forming a UO_{2+x} solid solution [Alberman and Anderson 1949, Aronson et al. 1957, Blackburn et al. 1958, Hoekstra et al. 1960, Walker 1965, Taylor et al. 1980, Einziger and Woodley 1985,1987]. These two mechanisms are difficult to distinguish by means of kinetic data [Hoekstra 1961, Einziger and Woodley 1987] and the details of the oxidation mechanism are still far from clear. Factors that could control oxygen diffusion would involve the relative stability fields of UO_{2+x} and U_3O_7, the growth kinetics of U_3O_7, the ratio of the diffusion coefficients in both phases etc. The rate law is not yet clear. Initial rates of UO_2 oxidation could be interpreted in terms of an exponential [Aronson 1957, Walker 1965, Einziger and Woodley 1987], a square root [Aronson 1957, Blackburn 1958, Walker 1965, Einziger and Woodley 1985] or a linear dependence on time [Tempest et al. 1988]. If film diffusion were involved, even a linear rate law would not contradict diffusion control.

The growth of a U_3O_7 surface layer on UO_2 may proceed to several microns of depth [Taylor et al. 1980, Simpson and Wood 1983, Tempest et al. 1988] into the UO_2 grains and result in stresses that cause intergranular and transgranular cracking but do not appear to cause gross disruption of the surface or spallation. The surface cracks serve as nucleation sites for the formation of initially isolated U_3O_8 mounds. The oxidation of U_3O_7 to U_3O_8 is sometimes preceded by an induction period which was explained by low rates of nucleation and growth of U_3O_8. Eventually spallation will occur in which whole grains become dislodged, leaving behind clean, unoxidized grains [Tempest et al. 1988]. Spallation and the production of particulate is a result of an increase in molar volume by 30% in connection with the transition from U_3O_7 to U_3O_8. One result of this process is that the specific surface area increases as a function of the degree of UO_2 oxidation [Blackburn et al. 1958, Smith 1960]. Results of Simpson and Wood [1983] indicate that once U_3O_8 is formed, the extent of oxidation is linearly dependent on time.

In order to evaluate the quantitative correlation between rates of oxidation in air and reaction rates of UO_2 in water, it is important to derive a diffusion coefficient for oxygen at room temperature from studies that are typically performed at temperatures of about 200°C (still called "low" temperature studies) or even at temperatures above 700°C. A general review of diffusion processes in UO_2 is provided by Matzke [1986, 1987] and D. Vollath [1986]. In the following literature data from both high- and low-temperature oxidation studies are compared and extrapolated to obtain a diffusion coefficient at room temperature.

III.2 Low-temperature oxidation data for UO_2 and spent fuel

Weight change results and rate constants from low temperature oxidation studies (120 to 300°C) of UO_2 and spent fuel were often used to describe the diffusion of oxygen quantitatively. The numerical value of a diffusion coefficient will depend on whether diffusion

through a surface layer of U_3O_7 or bulk diffusion is assumed. Since more than 30 years it is clear that weight gain data are not sufficient to distinguish between the two mechanism [Aronson et al. 1957, Einziger and Woodley 1987] and it is still uncertain which mechanism dominates. From X-ray evidence, Aronson proposed the matrix diffusion mechanism as the most likely case. Recent observations by Tempest, Tucker and Tyler [1988] clearly show the formation of a U_3O_7 layer. Still this does not exclude the matrix diffusion mechanism from being the rate controlling step.

Blackburn et al. (1958), Walker (1965) for UO_2 and Einziger and Woodley (1985) for low gas release spent PWR fuel interpreted the time dependence of weight gain in terms of a diffusion mechanism through a product layer of U_3O_7 using an equation of the form

$$1-(1-C)1/3 = \sqrt{k't}$$

or

$$r_o - r = \sqrt{2kt} \qquad (1)$$

where C is the fraction of UO_2 converted to U_3O_7, r_o is the radius of the unoxidized UO_2 solids, r_o-r is the thickness of the U_3O_7 layer and k or k' are rate constants which are related by $k'=2k/r_o^2$.

The rate constants are closely related to the diffusion coefficients in the U_3O_7 layer. A diffusion coefficient can be calculated by making an analogy with the growth of a film of tarnish on metal by rapid reaction with a gas [Crank 1955 p.117]. In application to UO_2 oxidation this would mean that the reaction proceeds by diffusion of dissolved oxygen through the U_3O_7 film to the surface of non-oxidized UO_2, where the concentration of excess oxygen is assumed to be zero. This is a moving-boundary problem in which the rate of movement of the UO_2/U_3O_7 interface is governed by the rate of oxygen diffusion in U_3O_7 and all diffused oxygen is consumed by the formation of U_3O_7. The position of the interface is given by

$$r_o - r = 2\alpha\sqrt{Dt} \qquad (2)$$

where α is given by the equation

$$C_o/W*\rho = \sqrt{\pi}\,\alpha\exp(\alpha^2)\,\mathrm{erf}(\alpha) \qquad (3)$$

where C_o is the concentration of dissolved oxygen in the outer surface, W is the mass fraction of excess stuctural oxygen in U_3O_7 and ρ is the density of U_3O_7. The product $W\rho$ gives the stoichiometrically constrained concentration of excess oxygen in U_3O_7. A diffusion coefficient can be calculated from the rate constants k or k' by combining Eqs.1 and 2 when the concentration C_o is known. If it is assumed that the concentration of oxygen free to migrate is given by the stoichiometry of U_3O_7, then $C_o/W\rho=1$ and α can be calculated to be 0.6 according to procedures given by Crank [1955]. Using this value, the combination of Eqs.1 and 2 yields a relation of a diffusion coefficient and a rate constant given by

$$D = k'r_o^2/1.44 \qquad (4)$$

In the spent fuel oxidation studies of Einziger and Woodley (1985) r_o is the radius of individual grains, because the authors determined k' for the situation where all grain boundaries are oxidized. In contrast in the studies of UO_2 oxidation [Blackburn 1958, Walker 1965] the grain boundary attack was neglected and r_o is equal to the sample radius.

As an alternative to layer diffusion, the matrix diffusion mechanism - involving formation of a solid solution of UO_{2+x} - has been used to interpret oxidation weight gain data by various authors (for spent fuel by Einziger and Woodley [1987] for UO_2 by Anderson et al. [1955], Aronson et al. [1957] and Walker [1965]). The time dependence of weight gain is usually [Aronson 1957] described by the formula

$$C = 1 - 6/\pi^2\,\Sigma(1/n^2)\exp(-\pi^2n^2Dt/r_o^2) \qquad (5)$$

where C is the fraction of UO_2 converted to U_3O_7, and D is the diffusion coefficient. Einziger and Woodley [1987] used the same equation but expressed the product $D\pi^2/r_o^2$ with the rate constant k. Conversion to a diffusion coefficient can be done directly.

Temperature dependent diffusion coefficients measured by the various authors are

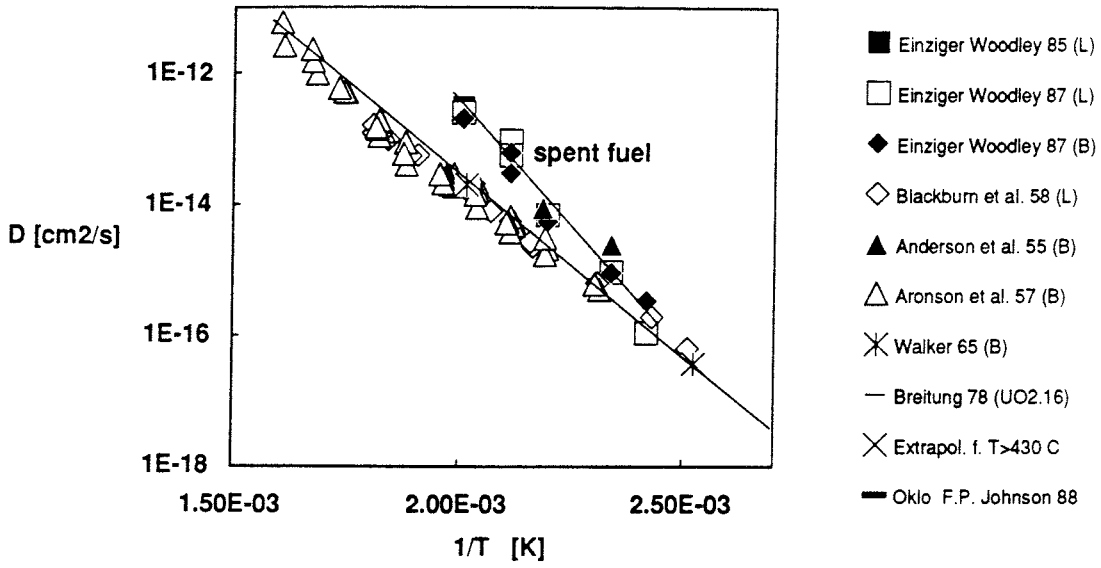

Figure 4: Compilation of diffusion coefficients for oxygen obtained from low-temperature oxidation studies of UO_2 or spent fuel performed at various temperatures

shown in Fig.4. Data interpreted by means of the layer mechanism are indicated by 'L' and those by the bulk diffusion mechanism by 'B'.

Coefficients for the bulk and layer diffusion mechanisms are identical within the uncertainty of the data. With only minor deviation from a straight line, all data for oxidation of UO_2 follow the temperature with an Arrhenius-type dependence. The activation energy is about 25 kcal/mol. Spent fuel oxidation seems to occur slightly faster than UO_2 oxidation, with a higher activation energy of 32 kcal/mol. With decreasing temperature, UO_2 and spent fuel oxidation become identical. Due to the high concentrations of defects, it is unlikely that oxidation rate of spent fuel will be lower than that of UO_2, so the activation energy of 32 kcal/mol should not be used for further extrapolation of the spent fuel curve to room temperature.

III. 3 Extrapolation of diffusion coefficients from high temperature data

In order to obtain a better understanding of the temperature dependence of UO_2 oxidation, the above-described bulk or layer diffusion coefficients for temperatures <350°C can be compared with results obtained at temperatures >500°C both for vapor oxidation [Bittel et al. 1969] of unirradiated UO_{2+x} and for reduction [Lay 1970] of UO_{2+x} in a hydrogen stream. The latter two experimental results can be mathematical represented by the general analytical expression for the diffusion coefficient of oxygen in a chemical gradient given by Breitung [1978]

$$\log D = A + 10^4 * B/T$$

for a temperature range between 500 and about 2500°C. The coefficients A and B used in the equation depend slightly (not as much as oxygen self-diffusion) on the stoichiometry of UO_{2+x}. For $0.0001 < x < 0.01$ the coefficients are A = -1.509 and B = -0.5227 and for x=0.16 A = -0.886 and B = -0.5409. The B values correspond to an activation energy of 23.8 kcal/mol or 24.6 respectively.

The activation energy for oxidation of $UO_{2.16}$ is very close to that obtained from low temperature oxidation studies, i.e. for diffusion in U_3O_7. A comparison of extrapolated high and low temperature data is given in Fig.5. Low temperature data are the same as those given in Fig.4. The extrapolated high temperature data are about two orders of mag-

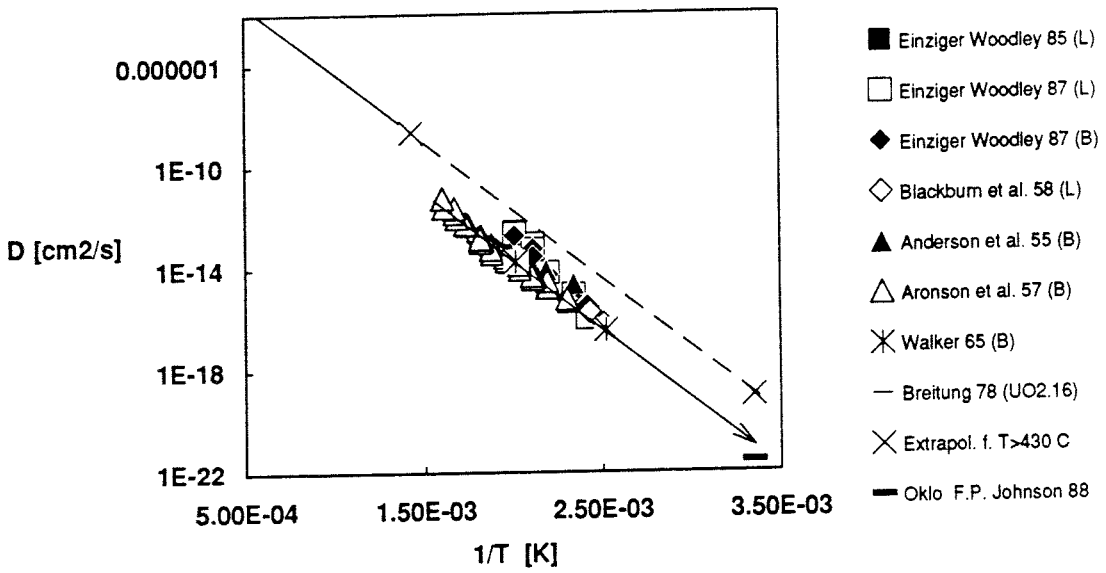

Figure 5: Comparison and extrapolation to room temperature of diffusion coefficients of oxygen in a chemical gradient obtained in low and high temperature studies . Data for fission product diffusion in the natural Oklo reactor are included for comparison

nitude higher than the diffusion coefficients obtained at low temperature. The discrepancy may be caused by the different stoichiometries (UO_{2+x}, $x < 0.16$ for $T > 500^{\circ}C$ and U_3O_7 for $T < 350^{\circ}C$). Such a decrease in the diffusion coefficient with an increasing value of x is the inverse dependence to what is known for lower deviations from stiochiometry ($x < 0.16$). A similar decrease was observed for oxygen self-diffusion when the oxidation state of the U_4O_9 field ($x=0.25$) was approached [Contamin et al. 1972, Murch et al. 1975].

In comparing the results from low and high temperature data, it may be concluded that an activation energy of about 25 kcal/mol can be used for extrapolation to room temperature.

However, in order to accurately extrapolate the observed temperature dependence of the diffusion coefficients, a better understanding of the discrepancy between the high and low temperature data would be necessarry. In this regard it would be useful to study diffusion coefficients of oxygen in U_3O_7. At present, diffusion coefficients at room temperature can only be estimated with large uncertainties. An upper limit can be estimated from values extrapolated from high-temperature data as

$D = 10^{-23}\ m^2/s$

and a value of

$D = 10^{-25}\ m^2/s$

can be estimated as a lower limit from the low temperature data.

III. 4 Diffusion coefficient of oxygen in grain boundaries of spent fuel

The above derived coefficients for bulk or layer diffusion describe the measured weight gain of the spent fuel grain matrix (T between 140 and 225°C, data from Einziger and Woodley [1985, 1987]). Penetration of oxygen into grain boundaries is much faster. It is likely that grain boundary oxidation can also be described as a diffusion process. If an easy access of oxygen to spent fuel grain boundary surfaces can be attributed to the presence of closely spaced fission gas bubbles along the boundaries, then the diffusion coefficient of oxygen and the rate of grain boundary oxida-

tion should depend significantly on the linear power rating of the fuel and the burnup.

For PWR fuel (27 MWd/kg U, 0.3% average gas release) Einziger and Woodley [1985, 1987] tried to quantify the grain boundary diffusion process based on data on the transient initial process, where the weight gain is lower than given by equation (1) or (5). Einziger and Woodley derived rate constants for this process. They assumed that the overall surface area for bulk matrix diffusion is proportional to the amount of oxidized grain boundaries. This hypothesis seems reasonable, as TEM work of Thomas et al. [1986] has shown that on spent fuel oxidation, grain boundaries are associated with multiple crack formation which may provide easy pathways for further oxidation.

The diffusion coefficient in grain boundaries is usually very difficult to assess because the grain boundary width, *a*, is generally unknown, and only the product D*2*a* is obtained from typical diffusion measurements [D. Vollath 1986, Olander 1986]. However, as the penetration depth of oxygen for a given diffusion coefficient does not depend on the width of the boundary, the study of the data of Einziger and Woodley may provide a unique opportunity to estimate a diffusion coefficient for oxygen in grain boundaries.

For grain boundary oxidation, Einziger and Woodley also used equation (5), but with a higher rate constant. Conversion of rate constants to diffusion coefficients can be performed again with $k=D\pi^2/r_o^2$, considering that the radius r_o of interest is no longer given by the grain size but by the fragment size (size of sample used is not reported but it may be estimated from its weight (200 mg) to about 2.7 mm, radius 1.3 mm). With these data the diffusion coefficient D for oxygen in grain boundaries is given within a factor of two of uncertainty

for 200°C $\quad D = 1.4*10^{-13}\ m^2/s$

According to Woodley et al. [1988] the activation energy for grain boundary oxidation is similar to that for matrix oxidation. With a value of 25 kcal/mol the diffusion coefficient is

for 25°C $\quad D = 2.3\ 10^{-20}\ m^2/s$

The value for the diffusion coefficient for grain boundary oxidation depends of course on the assumed transport mechanism. An alternative mechanism would be that diffusion of oxygen controls the rate only for the length of the boundary between two single grains. When oxygen has penetrated all the way along this grain boundary, the two adjacent grains may split from each other, due to the change in molecular volume of substrate and oxidized product, allowing easy oxygen access to the grain boundaries beneath. Such a process may in a first approximation be considered as repeated linearly with time as long as a large fraction of grain surfaces is not oxidized. In general, the diffusion coefficient for this mechanism would be expected to be smaller if used to interpret the same experimental data.

A diffusion coefficient for the diffusion/disruption mechanism may be calculated as follows. Einziger and Woodley [1985] reported the time at which grain boundary diffusion was completed as the time when grain matrix oxidation starts to follow a diffusional law. If that time (ca. 36 -100 h at 200°C) is devided by the number of grains (average grain size ø = 25 μm) within half the diameter of the fuel fragment sample (1.3 mm) then, with the assumption of a constant rate law, the time for oxidation of one boundary of adjacent grains can be calculated as tg ~ 1.3 h +- a factor of 2. Using this time a diffusion coefficient can be estimated with $D = \pi * \phi^2/4tg$ for 200°C as

$D = 10^{-13}\ m^2/s$ $\quad$ +/- factor of 2

and using again an activation energy of 25 kcal/mol the value for 25°C would be

$D = 1.7 * 10^{-20}\ m^2/s$

This means that within the uncertainty of the data, the dependence of the calculated diffusion coefficients on the transport mechanism may be neglected. If the values for the diffusion coefficient of oxygen in spent fuel grain boundaries are compared with the bulk

or layer diffusion coefficient in spent fuel at 200°C of about (Fig.4) $D = 5*10^{-17}$ m^2/s, it is found that diffusion in spent fuel grain boundaries is about four to five orders of magnitude faster than bulk diffusion. This difference is similar to that reported by Yajima [1966] and Hawkins et al. [1968]. The time, tg, of oxidation of a spent fuel grain boundary to a depth of the length of one grain diameter ø can be estimated at $tg = \pi * ø^2/4D$

If oxygen diffusion were governed by the coefficient, it would take about 800 years to penetrate into the fuel the distance of one grain diameter of 25 µm. Hence, grain boundary oxidation should be an extremely slow process at room temperature. Its effect would not be observable in any experiment. However, whether this is valid or not depends to a significant degree on the activation energies used for extrapolation, and since the actual activation energy for grain boundary oxidation is still not known, any extrapolation to room temperature remains highly speculative.

III. 5 Diffusion coefficients calculated from the release of soluble fission products from the natural Oklo reactor

Uraniferous rocks in the Oklo mines in the Republic of Gabon in equatorial Africa contain the wastes of natural fission reactors that were critical two billion years ago (Curtis [1985]). The natural reactor products were formed in-situ within the grains of uraninite, the promary host mineral for the natural waste. Grains of uraninite are dispersed in a clay matrix and are embedded in sandstone. More than 90% of the 'fuel' had remained at the same place it had been during criticality, showing the remarkable stability of uraninite under appropriate conditions. Actinides and rare earth elements stayed also largely in place, whereas Tc, alkali and alkali earth elements were released to the environment..

The principal mechanism for loss of fission products from the uraninite grains in the reactor core appears to have been very slow solid state diffusion. Diffusion coefficients for fission products in the uraninite grains were estimated acording to Cowan [1978] from the degree of retention of radionuclides in grains of known average radii. Johnson and Shoesmith [1988] used this method and estimated for Cs, Xe, Rb, Kr, Mo and Tc a diffusion coefficient of $1\text{-}4 * 10^{-26}$ m^2/s. A comparison with the data of Cowen [1978] shows that Sr and Ba have similar coefficients.

From the chemist's point of view it is rather surprising to find the diffusion coefficients of such chemically disparate elements so close together. A reasonable assumption is that the mobility of the various nuclides is governed by a common mechanism. In the light of the above discussions, oxygen diffusion seems to be the controlling process. The estimated diffusion coefficients for radionuclides can, therefore, be interpreted as diffusion coefficients for oxygen. The data have been plotted for comparision in Fig. 5. As can be seen, fair agreement is obtained between the extrapolated diffusion coefficient and the data from the Oklo reactor.

IV. EVALUATION OF CORROSION DATA FOR SPENT BWR AND PWR FUEL OBTAINED AT THE STUDSVIK LABORATORY

The data evaluation presented in this chapter focusses on the relationship between U-saturation in solutions obtained from spent nuclear fuel tests and the release of soluble radionuclides.

The corrosion of spent nuclear fuel has been studied at the Studsvik laboratory since 1977 [Eklund and Forsyth 1978]. Data were collected from tests with well characterized [i.e. Forsyth 1987] high burnup BWR (42 MWd/kg U) and PWR fuel (41.3 MWd/kg U) and with low burnup fuel (0.5 MWd /kg U) [Forsyth, Svanberg, Werme 1984; Forsyth, Werme, Bruno 1986; Forsyth and Werme 1985; 1987].

Briefly the experimental conditions can be summarized as follows: The test methods include static tests of almost three years' duration and two dynamic tests. Sequential tests (periodic renewal of leachants) are still in progress, the cumulative exposure time now being 6 years. Replenishment tests (periodical replacement of 20% of the leachant) were performed within a test period of less than a year. Most test specimens were 20 mm long segments (ca. 16 g UO_2) of fuel and clad cut out of the fuel rods at various positions. In some cases, various size fractions of fuel fragments were leached without the cladding present. Tests were performed in 250 ml pyrex flasks with 200 ml leachant at 20 to 25°C under oxidizing and reducing conditions. In the present evaluation only data from oxic conditions are considered. The leachants were either de-aerated deionized water or Allard water (for composition see Forsyth, Werme, Bruno [1986]). The contact volume of air was 50 ml. After the experiments, three parameters were analyzed: the soluble fraction of released radionuclides (1.8 nm filtrate), the material sorbed on or adhering to the vessel walls, and the material remaining on the filters. The analyzed radionuclides for high burnup fuel were U, ^{134}Cs, ^{137}Cs, ^{144}Ce, ^{106}Ru, ^{154}Eu, ^{90}Sr, ^{125}Sb, $^{239/240}Pu$, $^{241}Am/^{238}Pu$, ^{242}Cm, and ^{244}Cm. In the following evaluation only the data for ^{137}Cs, ^{90}Sr (or ^{89}Sr for low burnup fuel), ^{125}Sb, U and $^{239/240}Pu$ are considered.

The main results can be described as follows:

- U and Pu very rapidly reached saturation at neutral to slightly alkaline pH (1-2 mg/l and 1 ug/l respectively)
- the release rate of ^{90}Sr decreased with time but remained higher than the rate of U release
- the release of ^{90}Sr was similar in dynamic and static corrosion tests, hence, it was almost independent of the water "flow rate".
- for high-burnup fuel, congruent dissolution of soluble elements and U was observed only at pH values lower than 4
- the data for low-burnup fuel show a higher tendency towards congruent leaching behavior
- under reducing conditions, significant lower leach rates were observed
- BWR and PWR fuel show similar behavior
- no significant differences were observed between results from leach tests with fuel rod segments and with fuel fragments

IV.1 Solubility limits for the dissolving matrix under oxic conditions

It is a general result from spent fuel or UO_2 dissolution tests performed in the presence of atmospheric oxygen that the solution concentration of uranium reaches a constant value after short time periods. Although solution concentrations appear to be controlled by solubility equilibria with respect to some kind of oxidized phase, the solution concentration

may vary quite substantially during a long term experiment by as much as a factor of 100 [Ollila 1986]. For disposal of spent nuclear fuel, an important question is whether U saturation has any effect on the release rates of radionuclides. Saturation effects of silica in solution with respect to the dissolving solid play an important role in controlling the release of soluble radionuclides from nuclear waste glasses. It is important to study the potential of such effects in tests of spent fuel. A constant uranium concentration is not an unambiguous indicator of saturation effects with respect to the dissolving solid because constant uranium concentrations could also be a result of a steady state governed by the rates of dissolution and of precipitation, or could be controlled by the solubility of a secondary alteration product. Therefore, Shoesmith et al. [1988a] concluded that it is not possible to use a solubility-governed release model for fission products from spent fuel for oxic conditions. However, dynamic long-term experiments with BWR fuel [i.e. Forsyth and Werme 1985] seem to indicate that the release of soluble elements is affected by the solubility-limited release of uranium (see below). This indicates that uranium saturation may indeed affect the stability of the dissolving solid.

Initial attempts to identify the solubility controlling phase seemed to indicate that solution concentrations were in close agreement with the solubility limit of schoepite [Bruno et al. 1984]. This would agree with results from long-term experiments performed at 25°C with spent CANDU fuel in which UO_3*2H_2O (schoepite) was identified by XRD [Stroes-Gascoyne et al. 1985]. However, if the recently refined thermodynamic data for schoepite and for U(VI) hydroxo complexes at neutral to alkaline conditions are used it is found that uranium concentrations are about a factor of 30 lower than given by the solubility of schoepite [Bruno and Sandino 1988] (see also the calculation of even larger discrepancies given by Ollila [1988] when using another data base). Considering the large scatter of UO_2 solubility data under oxic conditions and the dependence of solubility on particle size [Bruno and Sandino 1988, Bruno and Grenthe 1988], this discrepancy may not be so surprising, but even if schoepite controlled the uranium release, the reason why the UO_2 dissolution rate (and the radionuclide release rates) decreases when it is formed would still have to be explained. Radionuclide release would only decrease as a consequence of schoepite formation when it constitutes a protective layer on UO_2. On the other hand, results of electrochemical experiments performed by Johnson et al. [1982] seem to indicate that a UO_3*xH_2O film is nonprotective.

Alternatively, the saturation effect with respect to the dissolving solid may be rationalized by electrochemical arguments consistent with the oxidative dissolution of UO_2. A general feature of an electrochemically controlled dissolution process is that the oxidation reaction (formation of UO_2++) and the reduction of the oxidant occur at different sites. The electrochemical potential at the surface may differ substantially from the overall redox potential in solution, which means that a potential gradient will be established and solubility calculations using bulk solution Eh data may be of no use for inferring the saturation state with respect to the dissolving solid.

Assessment of the solubility-controlling UO_2 surface potential

The electrochemical potential at the surface of UO_2 equals the open circuit potential, which was measured by various research groups for diluted conditions [Wang 1981, Sunder et al. 1981, 1987 Shoesmith et al. 1985] and which is also denoted as "corrosion potential" or as "mixed potential". This potential is to a certain degree independent of the bulk solution Eh because it is governed by the condition that anodic (dissolution) and cathodic (reduction of oxidant) currents must be equal when no external potential is applied. The potential dependence of anodic and cathodic currents and the corrosion potential are illustrated (Fig. 6) in a scheme taken from Johnson and Shoesmith [1988]. The interdependence of reduction of oxygen at cathodic

sites and dissolution of UO_2 at anodic sites may be described with an example given by the authors. If by any means (for example by using a catalyst) the cathodic current is increased (case 2 versus case 1), then the corrosion potential will shift to more positive values. As a consequence, the anodic current and hence the dissolution rate will increase.

In order to relate the surface potential of UO_2 to solubility constraints, it is necessary to understand the thermodynamic and kinetic factors that govern the corrosion potential. In principle both the anodic and the cathodic current can each be described by a combination of forward and reverse reactions, and far from equilibrium the reverse reaction can be neglected [Hiskey 1979]. A situation close to equilibrium is achieved when the equilibrium potentials of the two half reactions $UO_2 \rightarrow UO_2^{++} + 2e^-$ and $O_2 + 4H^+ + 4e^- \rightarrow 2H_2O$ are close [Shoesmith pers. communication]. The equilibrium potential for the anodic reaction is given by the equation [see Pourbaix]

$$(E_e)_a = (E^0)_a + 0.0295 \log UO_2^{++} \quad [V]$$

with E^0 calculated by $E^0 = (\mu^0_{UO2++} - \mu^0_{UO2})/2F$ from the recent data base of Bruno and Puigdomenech [1988] to be 0.325 V at 25°C. If the surface is partly oxidized, the E^0 value is higher. For the cathodic reaction the equilibrium potential for 25°C is given [Pourbaix] by the equation

$$(E_e)_c = 1.228 - 0.0591pH + 0.0148 \log pO_2 \quad [V]$$

These equations allow equilibrium effects to be distinguished from kinetic control of the corrosion potential. The equilibrium condition is given by $\Delta E_e = 0$ consistent with $\log pO_2 = 3.99\ pH + 3.99 \log (UO_2^{++}) - 39.05$. At 1 atm O_2 it appears to be rather unlikely that equilibrium can be attained, but it should be mentioned that this equation applies to surface concentrations. Due to the consumption of oxygen at the UO_2 surface the partial pressure of oxygen at the surface may be much lower than in solution, and despite disequilibrium with respect to the bulk solution local equilibrium is possible at the surface.

In order to identify the factors which control the corrosion potential, Fig. 7 shows the measured corrosion potentials from experiments by Shoesmith et al. [1985] in the presence of dissolved O2 and by Sunder et al [1987] in presence of H_2O_2 are compared with the results of thermodynamic calculations of the stability fields of various uranium oxides and of schoepite using the data base supplied by Bruno and Puigdomenech [1988]. Excluded from the data base was U_4O_9 be-

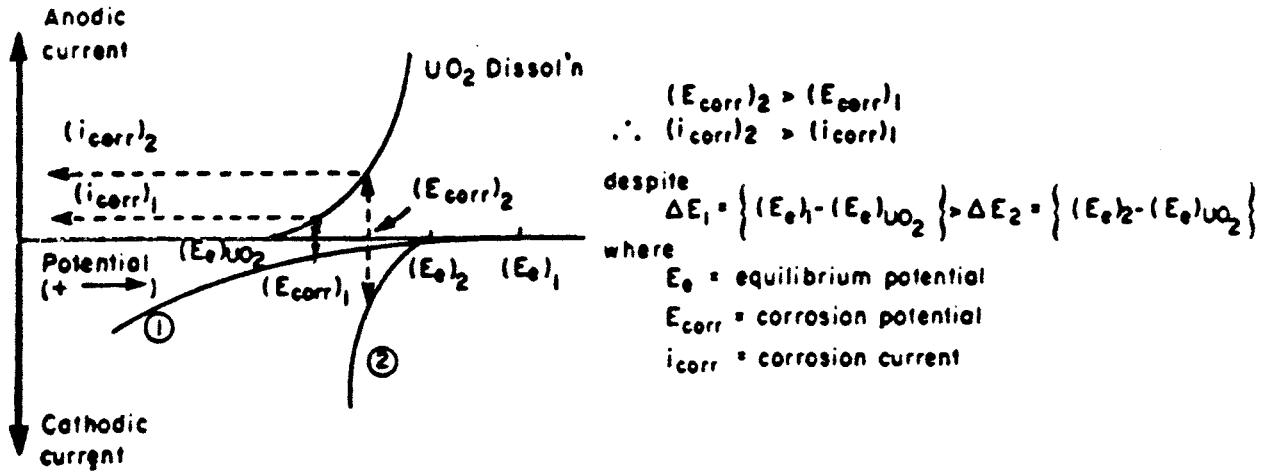

Figure 6: Scheme of an electrochemical interpretation of the dissolution of UO_2 fuel (taken from Johnson and Shoesmith [1988].

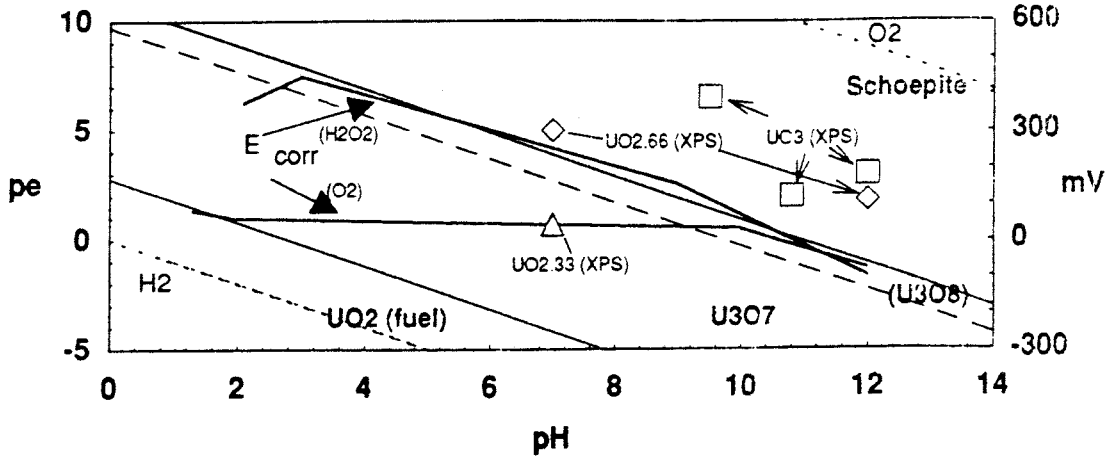

Figure 7: Comparison of the measured corrosion potential of UO_2 in the presence of dissolved O2 and in the presence of H_2O_2 [Shoesmith et al. 1985, Sunder et al. 1987] and XPS surface analysis results of UO_2 electrodes at certain applied potentials [Sunder et al. 1981, 1983] with results from thermodynamic calculations of the relative stability of various solids. "- - -" denotes the phase boundary U_3O_7/U_3O_8 in the unlikely event that the formation rate of U_3O_8 is fast enough and the solid line is calculated either for the UO_2/U_3O_7 or for the U_3O_7/schoepite boundary. XPS data give the highest oxide observed

cause U_4O_9 would be the most stable phase under mildly reducing conditions [Garisto and Garisto 1986], whereas there are indications that its formation at room temperature is kinetically hindered. For example, solution concentrations of uranium under reducing conditions remain oversaturated with respect to U_4O_9 for long periods of time [Bruno et al. 1987] and in UO_2 oxidation studies performed at low temperature direct transition from UO_{2+x} to U_3O_7 was observed and no U_4O_9 was detectable [Kuz'micheva et al. 1971]. At the oxidizing side of the UO_2 stability field two alternative phase boundaries were calculated, one for the situation when the formation of U_3O_8 would be too slow to control the dissolution of U_3O_7. In this case, the stability field of U_3O_7 is limited by the schoepite field. In the other case, the formation of U_3O_8 is fast enough to allow control at the U_3O_7/U_3O_8 boundary. The latter case appears to be rather unlikely as U3O8 formation is favored only under dry conditions [Shoesmith, pers. communication]. The diagram includes data for the highest oxides on the electrodes observed by Sunder et al. [1981,1983] for conditions where applied potentials were used. The comparison shows reasonable agreement between the observed surface oxide phases and the thermodynamic calculations.

The measured corrosion potentials seem to be closely related to the stability field of U_3O_7 (Fig.7). Three ranges of behavior can be distinguished, two where the corrosion potential follows the phase boundaries (at low pH UO_2/U_3O_7 and at high pH values either U_3O_7/U_3O_8 or U_3O_7/schoepite) and one in the stability field of U_3O_7, where the potential remains about constant. In the case, where H_2O_2 is present the pH dependence of the corrosion potential seems always to correlate with the U_3O_7/schoepite boundary.

At low pH (<2)the data indicate that the oxidation of UO_2 is fast enough to approach the stability field of U_3O_7. According to Sunder et al. [1985] the flat part of the corrosion potential curve at pH >2 in the presence of dissolved oxygen is governed by the relative rates of oxygen reduction and oxidative UO_2^{++} dissolution. Comparison with the thermodynamic calculations show that this flat part of the curve is located completely in the U_3O_7 stability field. This implies that the dissolving solid is not UO_2 but U_3O_7. In other words, U_3O_7 which is formed by diffusion of oxygen into the UO_2 lattice (see last chapter)

does form a "protective layer" on UO_2. This agrees with the interpretation given by Sunder et al. [1981] that under oxidizing conditions dissolution of UO_2 occurs from a surface oxidation state higher than given by the stoichiometry of U_3O_7. The protective nature of that film may be confirmed by surface analyses which show that U_3O_7 does not contain water (Matzke, pers. communication). If the dissolving solid is essentially U_3O_7 the equilibrium potential of the anodic reaction (see equation above) will shift towards more positive values when compared to pure UO_2. The anodic reaction may be described as

$$U_3O_7 + 2\,H^+ \rightarrow 3UO_2^{++} + H_2O + 4e^-$$

with

$$(E_e)_a = 0.384 + 0.0296pH + 0.0443\log UO_2^{++}$$

(E^o calculated with the help of the data base supplied by Bruno and Puigdomenech [1988]). As can be seen, an increase of both the pH and the concentration of UO_2^{++} will result in more positive equilibrium potentials for the anodic reaction and, therefore, a smaller difference to the equilibrium potential of the cathodic reaction (oxygen reduction), and at high pH values an approach towards control of the corrosion potential by equilibrium reactions cannot be excluded.

At pH values higher than 9.5 the corrosion potential seems to follow the U_3O_7/schoepite boundary given by the equation

$$Eh = 0.059 * (10.71 - pH).$$

corresponding to a log pO_2 value of -40.2. This correlation is an indication of a local equilibrium situation, although kinetic control is also possible (see below). A partial pressure of oxygen of $10^{-40.2}$ at the UO_2 surface indicates, on the other hand, that the electrode surface is not in global equilibrium with atmospheric oxygen. Disequilibrium with respect to atmospheric oxygen is quite common in natural water systems. If the UO_2-electrode surface is in local equilibrium with a solution phase at the surface, the corrosion potential will follow the phase boundaries in the event two solids are present in equilibrium with the same surface solution phase. According to the Gibbs phase rule, the solution concentration at the surface of uranium, log pO_2, Eh and pH are then no longer independent variables.

A univariant local equilibrium system does not rule out kinetic control of phase transformation. For example, if the rate of oxygen transport to the surface changes, the rate of phase transition will change without affecting the solution concentration of U and O_2 at the surface, and the surface potential. The equilibrium hypothesis implies a response of the surface oxidation state to the position with respect to the phase boundary. Indication of such behavior is provided by the XPS data of Sunder et al. [1981, 1983] (see Fig. 5) which show the presence of higher oxides at the oxidizing side (applied anodic potential) of the phase boundary and $UO_{2.33}$ at the reducing side. Recent results [Shoesmith et al. 1988b] of cathodic stripping voltammetry after initial open-circuit corrosion of UO_2 in air-saturated water indicate that a 6 nm thick film of $UO_{2.33}$ is formed at pH 9.5, and when the corrosion potential reached a value of 30 - 100 mV a small film of less than a monolayer was formed, which was attributed to UO_3*xH_2O. This behavior can be compared with Fig.7 and it can be concluded that when the corrosion potential reaches the phase boundary the U_3O_7 surface is covered partly with uranly hydrate. The thickness of this secondary film remained very small even after prolonged corrosion, indicating that the mass transfer rate of U_3O_7 to schoepite (UO_3*2H_2O) is low, as expected under saturated conditions.

The above thermodynamic interpretation of the slope of -59 mV/pH for the pH dependence of the corrosion potential is in conflict with the kinetic interpretation offered by Shoesmith et al. [1985] and Sunder et al. [1987] which suggested that this slope is controlled either by the rate of formation of the superoxide HO_2^- (in the presence of dissolved O_2) or in the case of peroxide being present, by the decomposition rate of H_2O_2. According to these arguments, the correlation of the corrosion potential with the phase boundary U_3O_7/schoepite is merely a coincidence, as is

the fact that the reaction rates of decomposition of peroxide and superoxide formation must be identical to explain the identical corrosion potentials in the presence of O_2 or H_2O_2 (Fig. 7).

Additional information in favor of the local equilibrium hypothesis stems from the reported variation of the corrosion potential with time [Johnson et al. 1982]. Initially, the open- circuit potential of an electrode cleaned cathodically at -2.0 V rose rapidly, the rate depending on the stirring of the solution. Then a plateau was reached and no further rise in potential was observed. Only these plateau values are plotted in Fig. 7. Although the occurence of such a plateau may still be explainable by kinetic reasoning, any such interpretation would also have to explain the overall time dependence of the corrosion potential. A more simple explanation seems to be that the plateau is governed by the univariant state at the phase boundary, and the increase in corrosion potential potential is governed by the decrease of the rate of UO_2^{++} detachment (anodic current, Fig. 6). It is revealing to compare the reported [Johnson et al. 1982] time dependence of the change in open-circuit potential at various pH values. In the presence of dissolved oxygen, the plateau is very pronounced at pH>9.5, i.e. when the corrosion potential is close to the phase boundary (Fig.7), whereas the plateau is only poorly developed at pH 2-5, i.e. when the corrosion potential is much lower than the boundary. In the latter case a further rise in potential cannot be excluded, but the experiments stopped prior to reaching a pronounced plateau.

Further evidence for univariant control of the corrosion potential at the phase boundary at pH>9 is the lack of influence of solution chemistry on the plateau potential, provided that enough oxygen is available. With and without the presence of carbonate, about the same plateau value of 0.1 V was reached at a pH of 9.5 [Shoesmith et al. 1988b]. Only the rates at which the plateau is reached change. With H_2O_2 these rates are about 200 times faster than in the presence of only dissolved oxygen [Shoesmith 1985]. This acceleration was attributed to the presence of OH radicals resulting from the decomposition of H_2O_2. In the presence of carbonate it takes longer to reach the plateau [Johnson et al.1982], since, due to the formation of solution complexes, more UO_2 must be dissolved before the phase boundary can be reached. The same plateau potential was reached in some cases even in N_2 saturated solutions, probably because traces of oxygen were present. It just took longer to reach the plateau, indicating that oxygen diffusion to UO_2 is rate-determining for the initial process [Johnson et al. 1982]. Under more carefully controlled conditions the corrosion potential plateau was lower when the system was degassed with N_2 [Shoesmith et al 1988b].

IV.2 UO_2 solubility under oxic conditions

There are saturation effects that affect the reaction rate and others that do not. The protective nature of the U_3O_7 film ensures that the dissolving solid is essentially U_3O_7, hence, when the solution becomes saturated with respect to this phase then the overall reaction rate may be expected to slow down considerably, as is the case of nuclear waste glasses and in agreement with transition state theory [Aagaard and Helgeson 1982]. Selective release of fission products from the UO_2 matrix is not possible without oxidation of UO_2 because in the fluorite structure of UO_2 oxygen is the most mobile species [Matzke 1986]. It is likely that for significant fission product release to occur, the degree of oxidation must go beyond U_3O_7, which defines the stoichiometric limit of the fluorite structure.

The solubility of U_3O_7 can be calculated if the Eh at the surface is known. Under air-saturated conditions above pH 9.5, the surface Eh may equal the corrosion potential given by the U_3O_7/schoepite boundary. At lower pH the situation is less clear, because the corrosion potential is much lower than the U_3O_7/schoepite boundary. Therefore, it is rather unlikely that schoepite will form at the

dissolving surface. Saturation effects would only involve U_3O_7. It is difficult to evaluate the effect on saturation of the disequilibrium situation between the solution phase at the surface and the bulk solution phase. Parallel to the gradient in the oxidation potential there should be a gradient in U solubility, with a higher saturation concentration in bulk solution than at the surface. Because of the resulting transport gradient for U from bulk solution towards the U_3O_7 surface, it is rather unlikely that saturation in the bulk solution will be reached (the solubility controlling phase at bulk Eh would be a U(VI) phase such as schoepite). An approach to U_3O_7 saturation may lead to a rise in the corrosion potential, because the equilibrium potential of the anodic reaction moves towards the equilibrium potential of the cathodic reaction (see Fig. 6). A maximum value for the corrosion potential under saturated conditions may be given by the U_3O_7/schoepite or the U_3O_7/U_3O_8 boundary. If the formation of U_3O_8 is kinetically hindered, as for solutions with pH > 9.5 or for solutions in contact with H_2O_2, the U_3O_7/schoepite boundary is favored, which is given at 25°C and 1 bar by the equation

$$Eh = 59.2 * (10.71 - pH) \quad [mV]$$

Under saturated conditions, at the U_3O_7/schoepite boundary, the surface solution concentration of U is fixed and the reaction rate equals the mass transfer rate from U_3O_7 to schoepite. An alteration product (schoepite) might be expected to act as a sink for U, which could enhance the corrosion rate of the dissolving solid and the release rate of soluble radionuclides [i.e. Garisto 1986]. However, such behavior is unlikely when the rate of phase transformation is controlled by an electrochemical process. Hypothetical increases in the UO_2^{++} detachment rates (increasing anodic currents), in conjunction with an unchanged potential dependence of cathodic current, would move the corrosion potential out of the stability field of schoepite into the U_3O_7 field and disturb the condition of alteration product formation (see Fig.6).

The present interpretation of U saturation in solution implies that no overall thermodynamic equilibrium is reached, but only a steady state. True thermodynamic equilibrium under oxidizing conditions would require complete converion of UO_2 and U_3O_7 to a higher oxide alteration product and finally to schoepite. In order to assess the steady-state mass transfer rates, it is important to study the effect of various oxidants other than oxygen (i.e. H_2O_2 produced by alpha radiolysis).

IV.3 Comparison of calculated U solubility with experimental data

Solution concentrations of U obtained in static, sequential and replenishment dissolution tests with PWR, BWR and low-burnup fuel in Allard water and in static tests with BWR fuel in deionized water [Forsyth, Werme 1986] were compared with the calculated saturation concentration of uranium in Allard water (synthetic granitic groundwater, composition: [Forsyth, Werme, Bruno 1986]). The calculations were performed using the geochemical computer code EQ3NR107 [Wollery 1983] with the uranium data base supplied by Bruno and Puigdomenech [1988] in conjunction with the EQ3/6 data base 3245R53. Various hypotheses for Eh control where tested. (1) The Eh was assumed to be given by the measured corrosion potentials (see Fig.7). Alternatively, the Eh was assumed to be given by (2) the U_3O_7/U_3O_8 or (3) the U_3O_7/schoepite boundary.

Depending on pH, Allard water may be sub- or supersaturated with respect to atmospheric CO_2. Hence, at the end of a long-term experiment, due to access of air, the CO_2 content may have been different than at the beginning. Therefore, two cases were calculated: one with the nominal HCO_3^- content of 123 mg/l and another, where the CO_2 content has been fixed by assumed equilibrium with atmospheric CO_2. Although calculated for Allard water the curve for atmospheric CO_2 is also applicable to deionized water experiments. The best agreement of calculated and ex-

perimental results was obtained for assumption (2). Good agreement between measurements and calculations was also obtained at values of pH of about 8 when the measured corrosion potential was used, but in the low pH range the calculated U solubility was much lower than the measured values (by up to a factor of 1000).

The results for the U_3O_7/U_3O_8 boundary are shown in Fig. 8. Calculations for the U_3O_7/schoepite boundary yield curves parallel to those described in the figure, the total concentration of uranium in solution always being about a factor of 30 higher (see also Bruno and Sandino [1988]). The scatter in the data is too great to give a final answer.

Excluding the data at low pH, the experimentally determined U concentrations are plotted as a function of cumulative contact time (Fig. 9). The data are compared with the calculated U solubility limit (U_3O_7/U_3O_8) for the nominal solution pH of Allard water of 8.2. A similarly good fit is obtained of U solubility calculated for an Eh given by the measured corrosion potential. As can be seen, most values fell in the range given by the difference between the solubility in the presence of atmospheric CO_2 and of the nominal CO_2. This could mean that the typically observed scatter in the U solubility data may result from a lack of control of the CO_2 content in the tests.

In order to compare the model with another set of data, U solution concentrations obtained from tests with unirradiated UO_2 at various concentrations of NaHCO3 were used [Ollila 1988]. Fig. 10 shows the results. Also given in the plot are the solubility curves calculated by Ollila [1988] with the help of the geochemical code PHREEQE [Parkhurst 1981]. At low carbonate concentrations there seems to be fair agreement between the new solubility interpretation and the data. At high carbonate concentrations the discrepancy becomes quite great. There are two possible explanations for the discrepancy. (1) The solutions at 600 mg/l of HCO_3^- are about 4 times oversaturated with respect to atmospheric CO_2, so solutions may have lost carbonate during the long duration (224 days) of the test. This interpretation is supported by experimental evidence showing that the pH rose during the test from an initial value of 8.5 to a value of 9.1. (2) The solutions with high carbonate content were not saturated. This is likely, because in the test at 600 mg/l HCO_3^- the solution concentration increased by almost a factor of 2 between 112 and 224 days.

The above evaluation can be summarized by

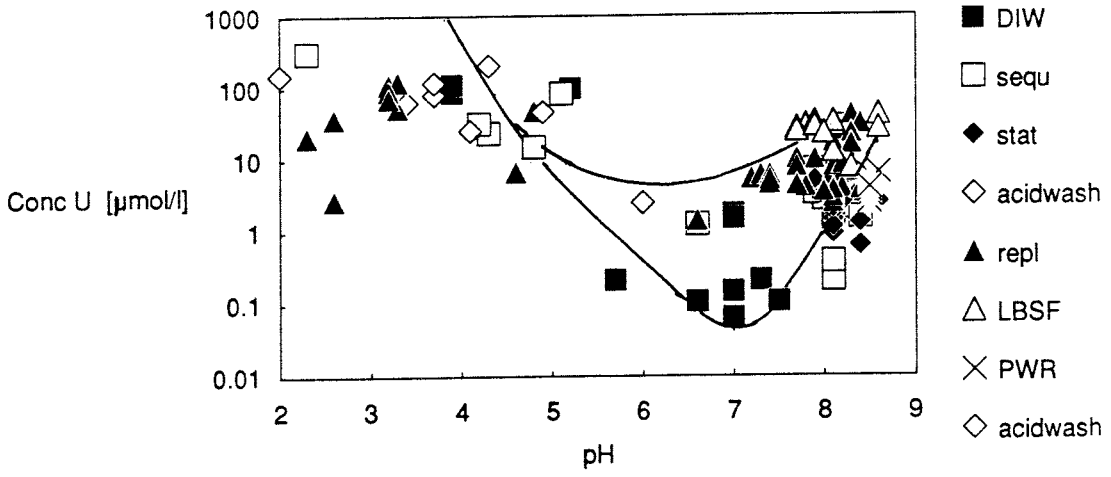

Figure 8: pH dependence of uranium concentration (µM) from corrosion tests with BWR fuel ("acid wash" = data from acid treatment of fuel after long-term static tests, DIW = static tests with deionized water, Allard water tests: Stat = static, repl = replenishment, sequ = sequential) PWR and low burnup fuel (LBSF) Comparison with calculated U solubility at the U_3O_7/U_3O_8 boundary. Upper curve: calculated for constant carbonate content, lower curve: carbonate control by equilibrium with air.

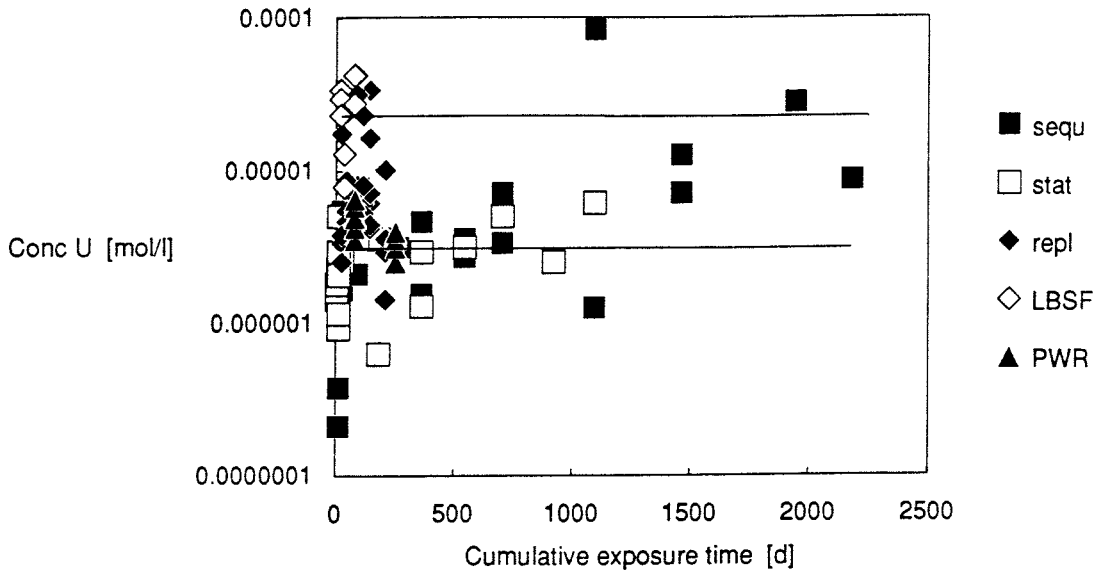

Figure 9: Uranium concentration (M) of spent fuel corrosion tests in Allard water (nominal pH 8.2) versus cumulative exposure time (key to symbols as in Fig.6). Comparison with calculated U solubility at the U_3O_7/U_3O_8 boundary at pH 8.2. Upper line: calculated for constant carbonate content, lower line: carbonate control by equilibrium with air.

stating that the the dissolving solid is essentially U_3O_7; hence, saturation effects with respect to this phase are important for the overall reaction rate. Solution concentrations of uranium in leach experiments with UO_2 under oxidizing conditions are similar to satuation concentrations at either the U_3O_7/U_3O_8 field boundary or at pH 8 at the measured corrosion potential. It should be mentioned that in the electrochemical experiments of Sunder et al. [1981-1988], the approach of U saturation was not studied explicitly. Such studies would be necessary for a further improvement of the interpretation of experimentally observed U saturation effects. A true thermodynamic equilibrium may never be achieved, because the surface potential at the U_3O_7 surface will remain lower than the potential given by the partial pressure of oxygen in the system. Determination of mass transfer rates for the conversion of U_3O_7 to higher oxide alteration products is very important, as U_3O_7 will most likely retain soluble radionuclides whereas higher oxides may not.

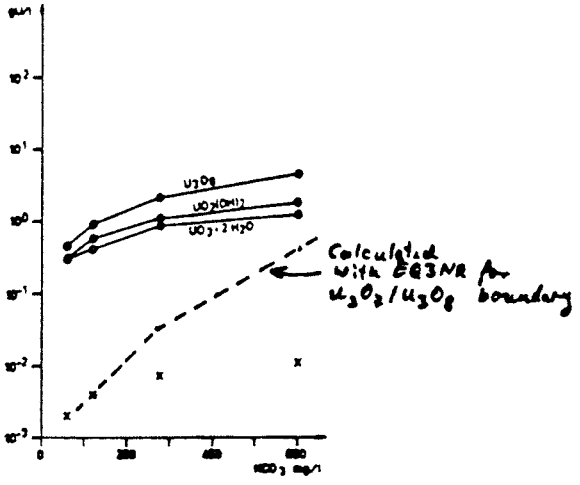

Figure 10: Comparison of unirradiated UO_2 solubility data (data and plot taken from Ollila [1988], solid curves obtained by the author from solubility calculations with PHREEQE) at various bicarbonate concentrations with calculated results for the U_3O_7/U_3O_8 boundary.

IV.4 Solubility limits for Pu

The fraction of the inventory of Pu in the aqueous phase (FIAP) is in most cases much lower than that of U, indicating solution control by the solubility of a precipitating phase, coprecipitation or sorption processes [Forsyth, Werme, Bruno 1986]. The solution concentration of Pu decreased with time. This was at-

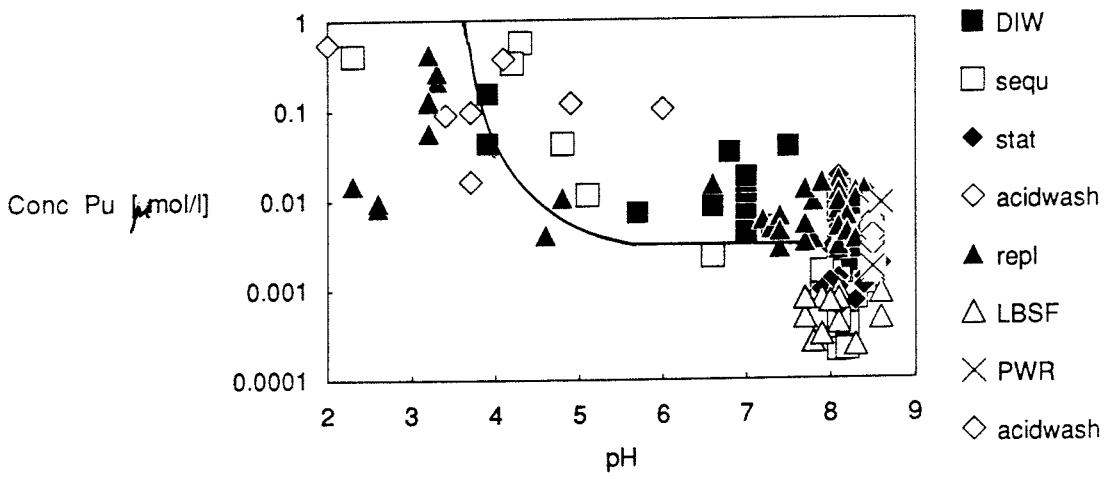

Figure 11: Comparison of Pu solution concentrations (inferred from $^{239/240}Pu$ activities) from spent BWR fuel dissolution tests (key to symbols as in Fig. 6) and a curve calculated with EQ3NR107 (database 3245R53) for solution control by $Pu(OH)_4(am)$ with the Eh controlled by the U_3O_7/U_3O_8 boundary.

tributed to the slow crystallization of an initially formed amorphous precipitate [FWB]. A comparison of solution data with the calculated solubility of PuO_2*xH_2O showed that the experimental data (5-8 nM; pH between 5 and 8.1) were about 2-3 orders of magnitude higher than the calculated values (0.01 nM). If PuO_2 (cryst) were used in the calculations, the expected solution concentrations would be a factor of 1000 lower. The most critical parameter seemed to be the solubility of the precipitating hydrolyzed plutonium oxide.

Recently [Bruton, Shaw 1987], the EQ3/6 code was used to calculate solution controls for Pu within a reaction path calculation for spent nuclear fuel. PuO_2(cryst) appeared to be the most stable phase and, therefore, this phase controlled the calculated release of Pu from the fuel. No attempt was made to consider the fact that the most stable phases are often also the most slowly forming phases. A Pu solution concentration of 0.001 nM was calculated, but if this calculation is repeated it is found that more than 99% of the solution concentration of Pu is tied to the species $PuO_2(OH)_2HCO_3^-$. The existence of this specie is rather unlikely [Grenthe, Robouch, Bruno, pers. commun.]. If it is excluded the solution concentration of Pu is more than a factor of 100 lower (10^{-14} M), i.e. more than 5 orders of magnitude below the experimental data.

An important question is which redox state to use for the calculations. Bruton and Shaw [1987] assumed equilibrium with respect to atmospheric oxygen. This is unreasonable, because solutions typically remain in disequilibrium with respect to oxygen for long periods of time. The above discussion of U solubility limits does show that a reasonable Eh is given neither by the oxygen partial pressure nor by the system's Eh but by the surface potential of the dissolving UO_2. Hence, when saturation with respect to uranium is achieved, Pu solubility must be calculated for the Eh at the U_3O_7/U_3O_8 or the U_3O_7/schoepite boundary. There is no difference in Pu(IV) solubility at both boundaries, because Pu(IV) species are in both cases dominant.

Using the EQ3NR107 code (data base 3245R53) the solubility of $Pu(OH)_4(am)$ was calculated for the Eh at the U_3O_7/U_3O_8 boundary as a function of pH, excluding the species $PuO_2(OH)_2HCO_3^-$. In Fig. 11, the calculated values are compared with the data from the spent BWR fuel dissolution tests. The total

concentration of Pu was inferred from the activity of $^{239/240}Pu$ in solution. As can be seen, there is reasonable agreement above pH 4. At lower pH values, it is likely that the solution concentration of Pu is controlled by kinetic constraints, i.e. by the dissolution rate of the UO_2 matrix. It is then, however, a contradiction that even in tests at low pH the Pu release was lower than the release of U.

In order to check whether the release of Pu could also be controlled by the release of U, the Pu to U ratio of the fractions of inventory in the aqueous phase is plotted in Fig. 12 as a function of cumulative exposure time. For tests in Allard water with low-burnup fuel and with high-burnup BWR and PWR fuel, the average ratio was 1/10, decreasing with time to almost 1/100. This seems to support the hypothesis of solubility control by crystallization of an initially amorphous hydrolysed plutonium oxide phase [Forsyth, Werme and Bruno 1986].

IV.5 Release of soluble radionuclides from spent nuclear fuel under U saturated conditions

For the dissolution of spent fuel under conditions typical for a repository, solubility control of the release of uranium is often considered to be a limiting factor for the release of those radionuclides that are more soluble than U as well.

An important factor is that, under oxidizing conditions, the spent fuel matrix is extremely unstable in thermodynamic terms. If the solubility-controlling phase for the observed U saturation concentration of about 1 mg/l is U_3O_7 or a higher oxide, then with respect to UO_2 a high driving force of reaction does remain (according to EQ3NR calculations, UO_2 is more than 10 orders of magnitude undersaturated). In principle, this would allow mass transfer of U from the UO_2 matrix to the higher oxide alteration products with the forward rate of reaction. This does not occur due to the two reasons described above: (1) U_3O_7 forms a protective layer on UO_2 and the dissolving solid is essentially U_3O_7. (2) Like UO_2, U_3O_7 retains the soluble radionuclides, because oxygen is by far the most mobile species in the fluorite structure [Matzke 1986, 1987]. In other words the release of soluble radionuclides depends on the dissolution of U_3O_7 and this dissolution process is solubility-limited.

The Studsvik data were used to further evaluate the dissolution of soluble radionuclides (^{90}Sr, ^{137}Cs, ^{125}Sb) from spent fuel under U saturated conditions. In order to facilitate a comparison with UO_2 dissolution

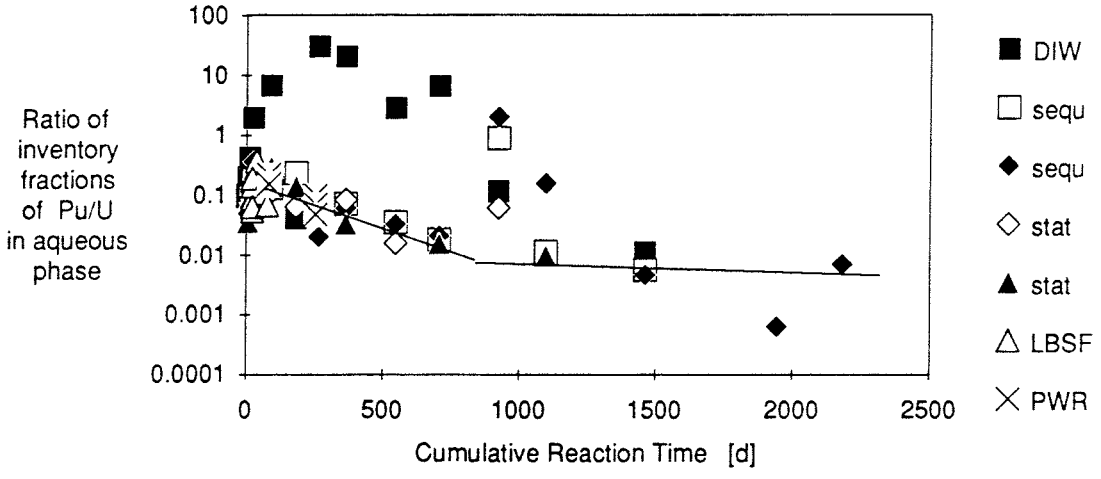

Figure 12: Time dependence of the Pu/U ratio of the fractions of inventory in aqueous phase (denotations of tests and materials as in Fig.8).

data reported in the literature (see chapter II) the release rate data were expressed as uranium dioxide equivalents in units of g/(m^2d) and not in the conventional units of "fraction of inventory in aqueous phase per day" [Forsyth, Werme, Bruno 1986]. The results are apparent reaction rates, and absolute rate data can only be obtained if the effective surface area is known. The assumptions used to obtain surface area are described in chapter II.3.

The apparent rate of release of soluble radionuclides generally decreases with time. The data do not allow direct study of whether the decrease of the release rate of soluble elements is an effect of U saturation, because solutions were generally saturated already after 14 days. A plot (Fig. 13) of the release rate of ^{90}Sr versus the solution concentration of U did not show any clear correlation. Yet there are some indications of an effect of U saturation on the stability of the UO_2 matrix and the release of soluble elements. For example, in a leach experiment with low-burnup BWR fuel U, ^{89}Sr and ^{137}Cs were released approximately congruently, and when U reached a constant concentration in solution, the rate of release of soluble elements decreased also (see Fig. 14 for ^{89}Sr and U). It should be mentioned that the straight line in Fig. 14 may indicate an initial corrosion rate under non - saturated conditions. This rate corresponds to 0.015 gU/(m^2d) and was used in the comparison of rate data in chapter II.3. Another, clearer example of the effect of saturation is the long-term experiment (up to 8 years [Stroes-Gascoyne et al. 1985, Forsyth, Werme 1985]) with periodic replacement of leach solutions. In these tests the rate of release of Sr resembles with time the rate of U release, and since the rate of U release is controlled by the U saturation concentration in solution and by the frequency of solution exchange, the similarity of Sr and U release means that U saturation controls the release of Sr as well, despite the fact that the UO_2 matrix is still very unstable thermodynamically.

In order to understand the decrease of the apparent Sr release rate for conditions where uranium has been saturated, the working hypothesis was made that Sr is distributed homogeneously in the UO_2 and U_3O_7 matrix (analogous to findings of Kleykamp [1985]) and that grain boundary segregation of Sr or (co-)precipitation or sorption of Sr does not occur. Since selective extraction of Sr out of the fluorite structure is not possible, the release data for Sr provide a lower limit for

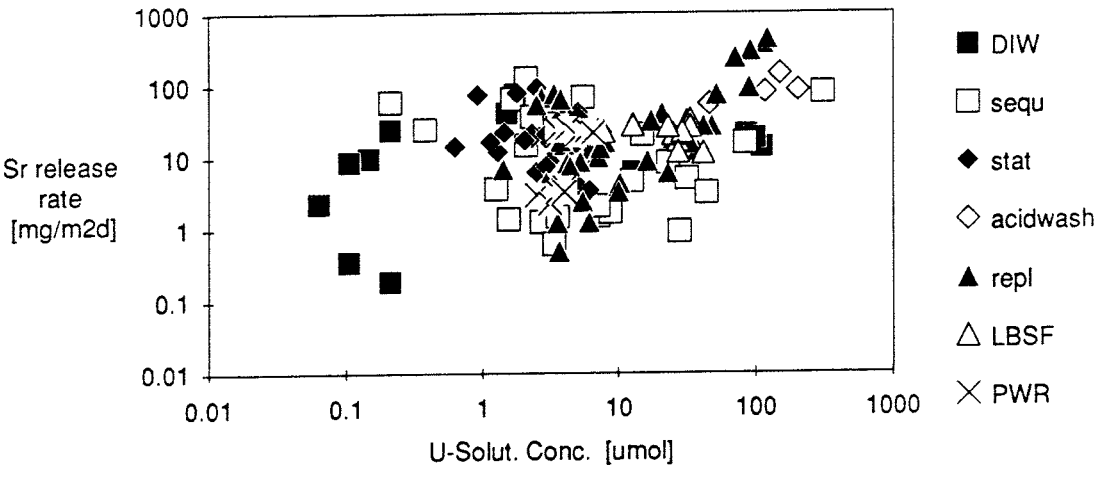

Figure 13: Correlation of the release rate [mg/(m^2d)] of ^{90}Sr from spent fuel tests with the U concentrations in the same tests, key to symbols as in Fig.8. Surface area used to calculate surface area normalized rates: 2 cm^2/g fuel

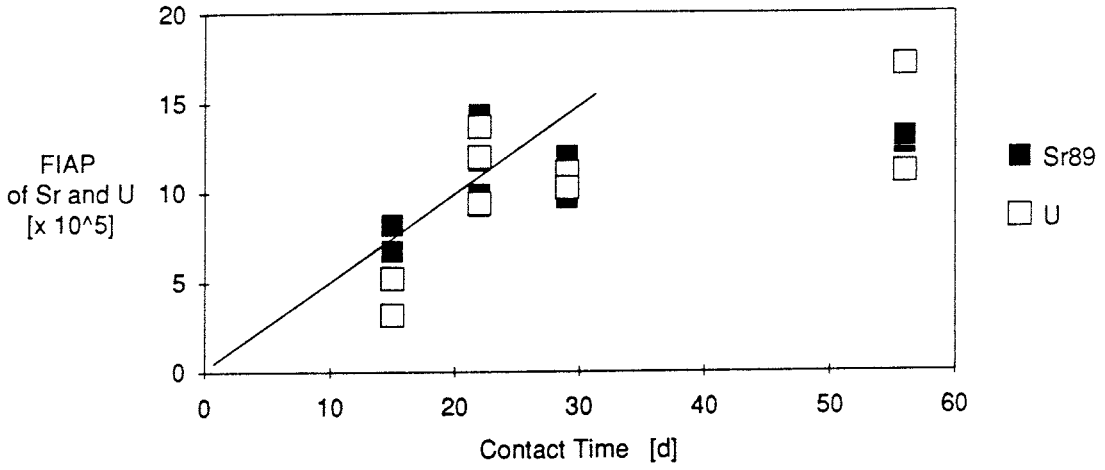

Figure 14: Fraction of inventory of ^{89}Sr and U in solutions ($*10^5$) resulting from tests performed at Studsvik with low-burnup fuel versus the contact time.

the degree of corrosion of the U(IV) matrix, i.e. the Sr data normalized to the inventory in the fuel equals the sum of U in solution and the mass of a solid alteration product (U_3O_8, schoepite). The difference between the fractions of inventory in aqueous phase (FIAP) of ^{90}Sr and U is, therefore, smaller or equal to the amount of UO_2/U_3O_7 converted to a solid alteration product. The total mass of alteration product formed was then calculated as a function of overall reaction progress from the difference between the cumulative Sr and U releases. Assuming that the alteration products remain as a surface layer on the fuel (the amount of U plated out is too small to account for the U deficit in solution) an average layer thickness can be calculated, provided that the specific surface area of the fuel is known. Since grain boundary oxidation and/or fission product segregation may allow water access to grain boundaries, the effective specific surface area will be between the geometrical surface area and the surface area of separated grains. The total surface area of individual grains is about 200 times higher than the geometrical surface area, and therefore the uncertainty in the calculated layer thickness is given by this factor 200.

For the experiments performed at Studsvik with BWR and PWR fuel under oxidizing conditions (static, sequential and replenishment tests, [Forsyth, Werme 1986]) Fig. 15 shows a plot of the apparent depth of an oxidized surface layer as a function of the square root of the total exposure time. The plot reveals a consistent trend in all of the data which is best represented by a straight line indicative of a rate-controlling transport process. Between 20 and 2000 days none of the data for high-burnup PWR and BWR fuel deviated by more than a factor of two from the line.

There are at least five possible explanations for the dependence of the growth of an apparent alteration products layer on the square root of time. (1) It is a real layer and diffusion processes through this growing layer of higher oxide alteration products control the dissolution rate of UO_2/U_3O_7. (2) Oxygen diffusion through UO_2/U_3O_7 controls the rate. (3) The main transport path is not volume diffusion but diffusion in grain boundaries. (4) The assumption of homogeneous distribution of Sr in the grains is wrong, and Sr is enriched at the grain surfaces with a diffusion profile that gradually dissolves as the UO_2 matrix dissolves. (5) Segregation of Sr in the grain boun-

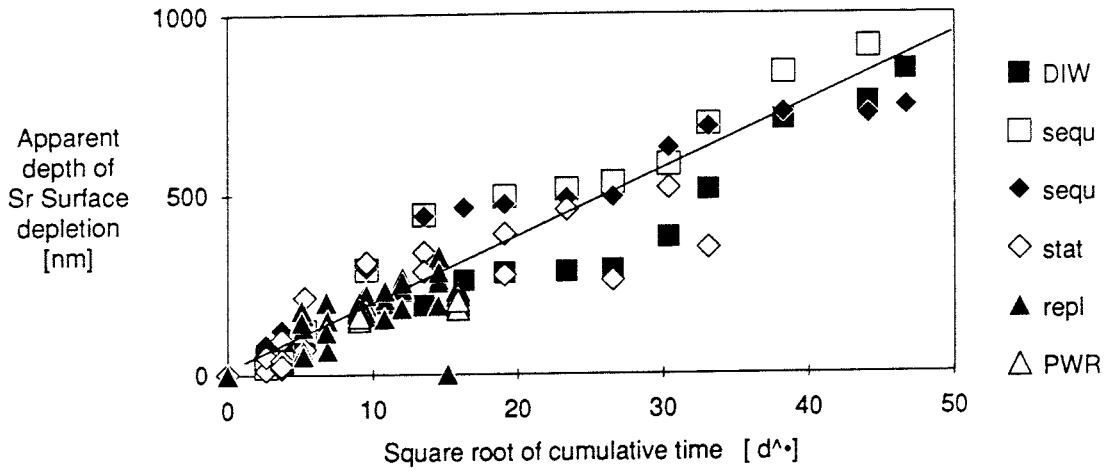

Figure 15: Time dependence [d] of the difference of the apparent cumulative corrosion depth [nm] of ^{90}Sr and U as calculated from release data of high burnup BWR and PWR fuel in static, replenishment [repl] and sequential leach tests with deionized water (DIW) and synthetic ground- water [sequ]. Data are arbitrarily normalized to an estimated specific geometric surface area of fuel fragments of 2 cm^2/g fuel.

daries cannot be neglected and grain boundary diffusion is the controlling process. Explanations (1) to (3) can be distinguished from (4) and (5) by studying the behavior of other soluble elements. Fig. 16 and 17 show plots similar to Fig. 15 but for ^{125}Sb and ^{137}Cs. For ^{137}Cs the data from the first contact with the solution were not considered because initially a high amount of ^{137}Cs is released from the gap. For ^{125}Sb the data do not show a clear trend. Only in one sequential test series there was some indication for a square root of time dependence. For ^{137}Cs the data are consistently higher than the Sr data, but in the sequential tests the square root of time dependence is even clearer. The offset in the curves is probably due to the fact that gap-release is not yet completed. A higher Cs release is a generally observed fact, and if gap release is completed it may be attributed to leaching of Cs-enriched grain boundaries. The trend in the data from the static tests is not clear because the scatter in the data is high. The large scatter may be caused by different amounts of non-completed gap-release included in the data after excluding the major fraction of gap-release when preleaching the samples for 14 days.

If diffusion through a growing surface layer limits the rate of Sr release under oxidizing and U saturated conditions (case 1) than there are two further options. (1a) A surface precipitate is forming and (1b) higher oxides grow by pseudomorphic replacement of UO_2/U_3O_7 and Sr release may occur through a growing oxidized zone. Surface precipitates such as rutherfordine in high-carbonate solutions are often found to reduce the dissolution rate of unirradiated UO_2 or limit the anodic currents of UO_2 electrodes [Nicol and Needs 1977, Wang 1981, Ollila 1988] with respect to the rate under subsaturated conditions. However, there are also conditions where surface precipitates do not limit the reaction rate [Wang 1981]. Case 1b would be in agreement with surface oxygen profiles reported by Wang [1981]. No information is available on the diffusion of Sr, water and oxygen in higher oxides, but the validity of cases 1a and b rests with slow transport processes. On the other hand, the discussion of solubility controls for U (chapter IV.1) has provided indica-

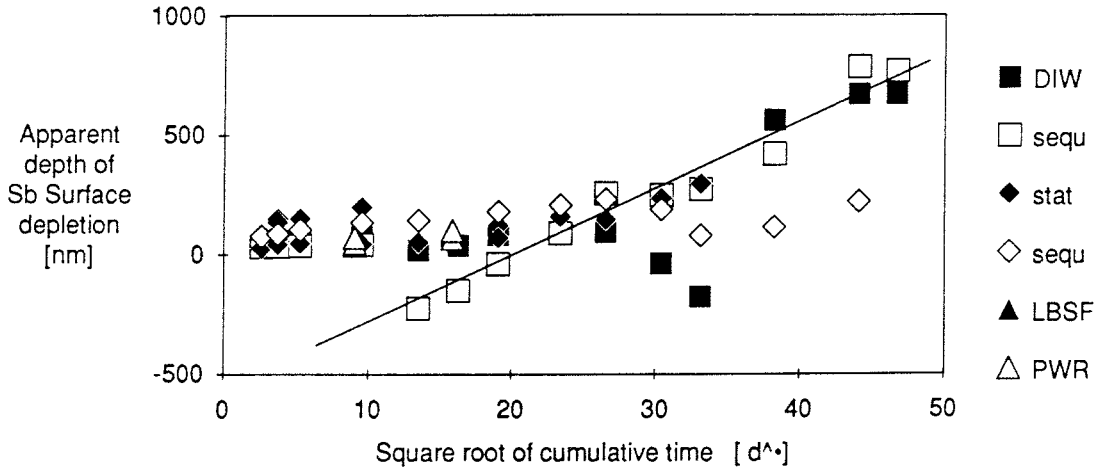

Figure 16: as in Fig. 15 but ^{125}Sb data

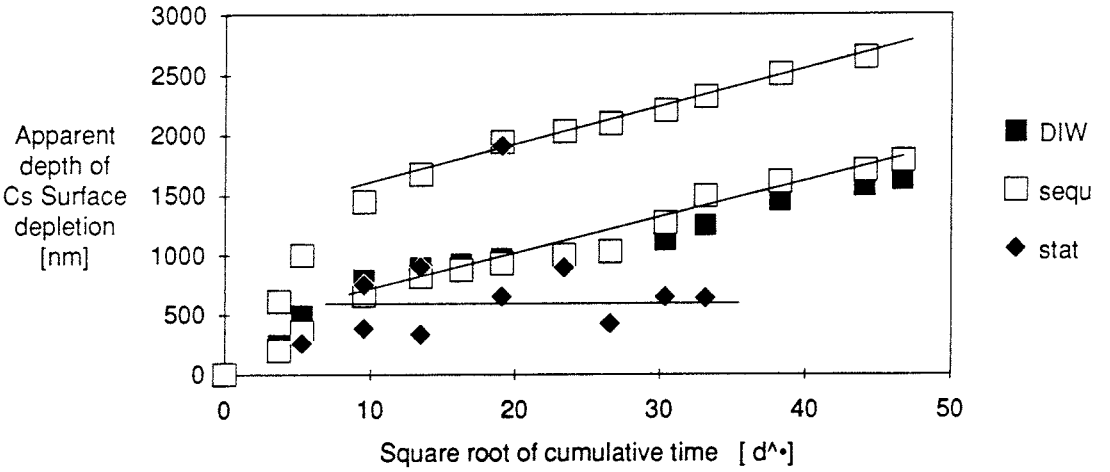

Figure 17: same as Fig. 15 but ^{137}Cs data

tions that U_3O_7 has direct contact with the aqueous phase. This would either mean that transport through higher oxides or schoepite is fast or that the phases are separated by a gap. If those transport rates are fast, oxygen diffusion in a chemical gradient of hyperstoichiometric UO_2 (up to U_3O_7) may be the limiting factor (case 2) for the formation of U_3O_8 and/or schoepite and for the release of soluble elements.

In order to test this hypothesis, the diffusion coefficient of oxygen in a chemical gradient in UO_2 can be compared with a diffusion coefficient obtained from the straight line in Fig.

15. The diffusion coefficient of oxygen is rather uncertain at room temperature. It was extrapolated from available high-temperature data (see discussion chapter III) to obtain a value of 10^{-24} m^2/s. For Sr release from spent fuel, the value of a diffusion coefficient can be calculated from Fig. 15 with the help of the formula $D= \pi/4*x^2/t$ where x is the apparent depth of the oxidized layer at time t. With x also D depends on the assumed effective specific surface area. Using the geometrical surface area a D value of $4*10^{-21}$ m^2/s is obtained. If all grain surfaces are accessible to water, the value is 10^{-25} m^2/s. There seems to be agreement with the diffusion coefficient for oxygen in a chemical gradient. The diffusion coefficient from Fig. 15 is equal to the extrapolated diffusion coefficient for oxygen diffusion when grain boundaries of 15 layers of grains, counted from the surface of a fuel fragment, are accessible to oxygen-containing water. This seems to coincide with reported SEM micrographs of leached spent fuel surfaces which show open grain boundaries several grain diameters in length. Under such conditions, the average thickness of an oxidized layer would be 7 nm after 2000 days. There seems to be the possibility of surprising agreement between the Sr release data, structural information and diffusion data for oxygen in UO_2/U_3O_7.

V. SOME THOUGHTS WITH RESPECT TO A MODEL FOR OXYGEN DIFFUSION AND THE RELEASE OF SOLUBLE FISSION PRODUCTS IN DISSOLVING SPENT FUEL UNDER U SATURATED OXIC CONDITIONS

In the following, some steps in developing a model for spent fuel dissolution under oxidizing conditions are discussed. A generally applicable model would have to consider seperately the chemistry of grain boundary oxidation/dissolution and of the dissolution of exposed surfaces. Some experiments with fuel of different surface-to-solution-volume ratio are needed which would determine whether the release of fission products is proportional to surface area or whether surface area is not a critical factor due to solubility constraints. If the effective surface area is of importance for the release of fission products, then the time dependence of the total wettable surface area may have to be considered. Due to diffusion-controlled grain boundary oxidation/dissolution, the overall surface area will increase with time. The grain boundary oxidation and dissolution process may be quite complicated, since the stage of reaction progress per unit volume at grain boundaries may differ substantially from that at exposed surfaces. This is due to volume restrictions, where voluminous high-oxide phases (U_3O_8, schoepite etc.) can only form when grain boundaries are ruptured or when open grain boundary porosity is present due to fission product segregation. Volume reduction by the formation of U_4O_9 or U_3O_7 may be a necessary condition for the formation of small amounts of higher oxides in grain boundaries. In other words, the equilibrium redox potential between U_4O_9 or U_3O_7 on the one hand and higher oxides on the other is shifted in grain boundaries towards more positive values (see the pressure dependence of the equilibrium constant as a function of the change in the apparent molecular volume of the reaction).

Using the observed apparent correlation between the diffusion coefficient of oxygen in UO_2 and the release of fission products a schematic model can be outlined in which the release of soluble fission products is proportional to the degree of fuel oxidation.

A model was designed similar to the description of alkali ion exchange on glass surfaces for moving boundary conditions [Doremus 1979, Boskay 1967] for illustrative purpose. A development of the mathematics of the model is described in the quoted reference. It is assumed that the solution is saturated with respect to a secondary alteration product and the fuel matrix dissolves at a constant rate, which is zero under static conditions and is given by the product of flow rate and saturation concentration under dynamic conditions.

For the outer surface of the fuel a fixed UO_3*xH_2O composition is assumed for the sample calculations. No attempt is made to account for possible phase boundaries between various oxides that form along the diffusion path (U_4O_9, U_3O_7, U_2O_5, U_3O_8) and since no diffusion coefficients for oxygen and/or water in the higher oxides were available, no allowance is made for the effect of the more open structure of the higher oxides on oxygen transport. For the release of soluble fission products such as ^{90}Sr, ^{125}Sb or ^{137}Cs two cases were calculated. It was assumed that Sr is released proportionally to the oxygen uptake of the surface. Hence, the depth profile of Sr depletion should match the inverse oxygen penetration profile. As this would also assume the unlikely release of a fraction of radionuclides from the UO_2 or U_3O_7 structure, a more realistic case (not yet calculated) would be when fission product release is only allowed when the oxygen content of the surface is higher than given by the composition of U_3O_7. Support for this latter case is provided by the electrochemical studies of Shoesmith et al. [1981], which show that for U(VI) subsaturated systems dissolution of UO_2 starts when a surface composition of U_2O_5 has been reached. Under the U(VI) saturated conditions considered here the dissolution of U cannot occur, but radionuclides

may still be released. A list of model parameters is given in table 2.

Table 2: List of model parameters typical for a sequential corrosion test

groundwater flow rate	F = 1.1 ml/day
U(VI) saturation conc.	CS = 2 mg/l
density of UO_2	d = 10.35 g/cm^3
molecular weight of UO_2	MG = 270 g/mol
atomic weight of U	AG = 238 g/mol
geometric surface area	SG = 32 cm^2
assumed number of water accessible grains per surface grain	N=5
water accessible surface	S = SG * N * 6
corrosion rate	a = F*CS*MG/(S*d*AG)
O_2 diffusion coefficient	D = 10^{-24} m^2/sec
concentration of transportable oxygen at outer surface	C_o = 38 mol/l

The following equation yields the average valence state 'val' (between 4 and 6) of uranium at a distance y from the surface. The surface retreats into the fuel matrix at a rate, a. Using the abreviations

$$s(y,t) = y-at/2\sqrt{Dt} \qquad g(y,t) = y+at/2\sqrt{Dt}$$

the valance state is given by

$$val(y,t) =$$

$$4 + erfc(g(y,t)) + exp(-ay/D) *erfc(s(y,t)).$$

A plot of the valence state of the surface as a function of depth after 3 years of oxidation is given in Fig. 18.

Assuming that the release of fission products from the fuel is controlled by the degree of surface oxidation, the rate of release of ^{90}Sr from the fuel is given by the following equation. The rate is expressed in terms of equivalent grams of uranium release per unit area of the surface.

$$r_{Sr} = MG*(C_o*a/2*(1+1/2erfc(s(y,t))) +$$

$$C_o(D/\pi exp((-s(y,t)^2))$$

In Fig. 19 the time dependence of the rate of release of Sr is compared with the rate, r_u, of release of U. Initially, the rate of Sr release is more than a factor of 100 higher than the rate of release of uranium, but with time the rate of Sr release approaches that of uranium. After about 4 years of reaction, the release rate of Sr is only 3 times higher than that of uranium.

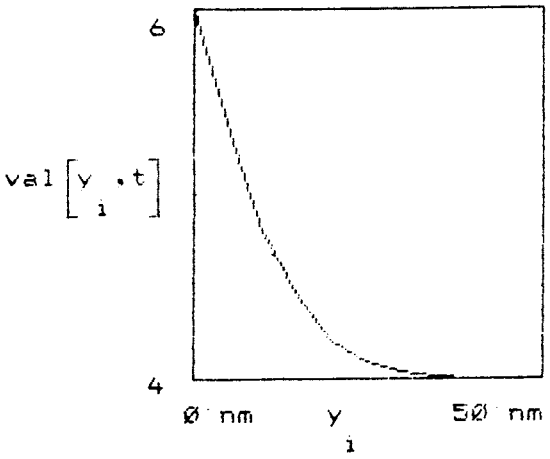

Figure 18: Average valence state of uranium on a UO_2 surface after 3 years of oxidation.

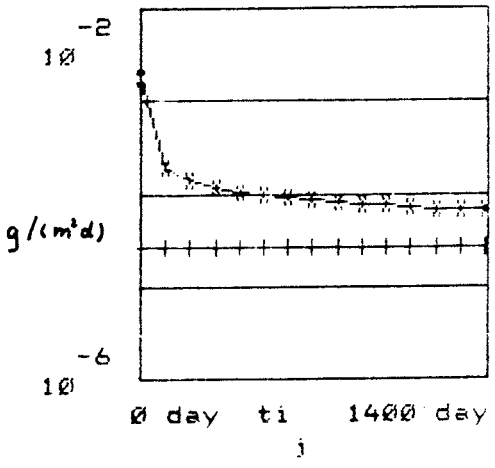

Figure 19: Normalized release rates of Sr (xxx) and U (+++) from spent fuel as a fucnction of time in a dynamic leach test

In Fig. 20 the release of Sr and U per surface area from the fuel is expressed in terms of an equivalent reaction depth D_{Sr} and D_U. The depths D_U and D_{Sr} are given by the formula

$$D_U = r_u * t / d$$

$$D_{Sr} = r_u * t/d + \int(1+(val(y,t)-6)/2)dy$$

A total depth D_O of oxidized fuel remaining on the surface is given by $D_O = D_{Sr} - D_U$.

The results of the double logarithmic plot in Fig. 18 show that with time the rate of Sr release becomes slower (due to oxygen diffusion through an increasing layer thickness) and, for the conditions assumed, after about 300 years a steady-state layer thickness (here about 50 nm) will be achieved when the rate of oxygen diffusion equals the rate of UO_2 dissolution. The time at which steady state is reached depends on the water flow rate, the oxygen diffusion coefficient and the effective surface area. Therefore, the numeric results calculated in the present example may be of no meaning in a more realistic calculation.

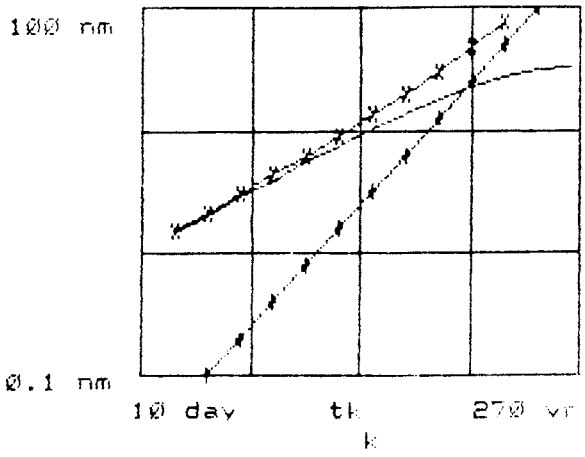

Figure 20: Average depth of Sr (xxx) and U (+++) release from water-accessible spent fuel surface grains (relative to the initial outer surface plane) and average thickness (___) of the oxidized surface layer as a function of time

Nevertheless it is important to note that, as was found in the sequential leach tests performed at Studsvik, the model states that at longer reaction times the release rate of Sr seems to resemble the release rate of U.

Acknowledgement

The major part of this report was written during a three month visit at the Royal Institute of Technology in Stockholm, Sweden. In particular, wish I to thank Dr. J. Bruno and his group for their kind hospitality. I would like to acknowledge Dr. J. Bruno, Prof. I. Grenthe and Dr. D. Shoesmith for carfully reviewing parts of or the whole manuscript. The work was sponsored by SKB/Stockholm.

REFERENCES

AAGAARD P., H.C. HELGESON, "Thermodynamic and Kinetic Constraints on The Reaction Rates Among Minerals and Aqueous Solutions, I. Theoretical Considerations" Am. J. Sci. 281, pp 568-610, (1982)

ALBERMAN K.B., J. S. ANDERSON, J. Chem. Soc. (1949), 5303

ALLEN G.C. and P.A. Tempest, "Linear Ordering of Oxygen Clusters in Hyperstoicheiometric uranium Dioxide", J. Chem. Soc. Dalton Trans. pp. 2169-2173, 1982

ALLEN G.C., "An angle-resolved X-Ray photoelectron spectroscopic study of air-oxidized UO_2 pellet surfaces", Philosophical Magazine B. 51 (4), (1985) 465-473

ALLEN G.C., P.A. TEMPEST, J.W. TYLER, "Oxidation of Crystalline UO_2 studied using X-Ray Photoelectron Spectroscopy and X-Ray Diffraction", J. Chem. Soc. Faraday Trans. I. 83 (1987) 925-935

AMELL A.R., D. LANGMUIR, "Factors Influencing the Solution Rate of Uranium Dioxide Under Conditions Applicable to In-Situ Leaching". Bureau of Mines Open File Report 84-79, United States Department of the Interior - Bureau of Mines (1978)

ANDERSON J.S., L.E.J. ROBERTS, E.A. HARPER, "The Oxides of Uranium. Part VII. The Oxidation of Uranium Dioxide", J. Chem. Soc. (1955) 3946-3959

ARONSON S., "Oxidation of UO_2 in Water Containing Oxygen". Bettis. Tech. Rev. Westinghouse Atomic Power DIV., Report WAPD-BT 10 p.93, 1958.

ARONSON S., ROOF R., BELLE J., Kinetic study of the oxidation of uranium dioxide. J. Chem. Phys. 27, 1, 1957

ARONSON S., "Oxidation and Corrosion of Uranium Dioxide, in 'Uranium Dioxide: Properties and Nuclear Application'", J. Belle ed., United States Atomic Energy Commission, 1961

BITTEL J.T., L.H. SJODAHL, J.F. WHITE, J. Amer. Ceram. Soc. 52 (1969) 446-51

BLACKBURN P.E., "Oxygen Pressures over Fast Breeder Reactor Fuel - (I) A model for UO_{2+x}", J. Nucl. Mater. 46 (1973) 244-252

BLACKBURN P.E., J. WEISSBART, E.A. GULBRANSEN, "Oxidation of Uranium Dioxide", J. Phys. Chem. (1958) 902-908

BOKSAY, Z., G. BOUQUET and S. DOBOS, "Diffusion Processes in the Surface Layer of Glasses", Phys.Chem.Glasses, 8, 4, pp. 140-144, (1967)

BREITUNG W., "Oxygen Self and Chemical Diffusion Coefficients in UO2+-x", J. Nucl. Mater. 74 (1978) 10-18

BRODDA B., MERZ E., "Leachability of actinides and fission products from spent HTR fuel", Presented at the Workshop Migration 87, Munich 1987

BRUNO J., I. CASAS, I. PUIG-DOMENECH, "The Kinetics of Dissolution of UO_2(s) Under Reducing Conditions", Radiochimica Acta, 1988

BRUNO J., et al., Fysisk-kemiska undersökningar och matematisk modellering av det använda bränsletsupplösningen, Kvartalsrapport 88-01-19, Royal Institute of Technology, 10044 Stockholm, 1988

BRUNO J., I. PUIGDOMENECH, "Validation of the SKBU1 Uranium Thermodynamic Data Base for its Use in Geochemical Calculations With EQ3/6", presented in 'Scientific Basis for Nuclear Waste Management XII', Berlin 1988

BRUNO J., A. SANDINO, "The Solubility of Amorphous and Crystalline Schoepite in Neutral to Alkaline Solution", presented in Scientific Basis for Nuclear Waste Management XII, Berlin 1988

BRUNO J., R.S. FORSYTH, L.O. WERME, "Spent UO2-fuel Dissolution, Tentative Modelling of Experimental Apparent Solubilities", Mat. Res. Soc. Symp. Proc. Vol. 44, Materials Research Society, Pittsburgh, PA 15237, pp. 413-420 (1984)

BRUNO J., I. GRENTHE; "A Reinterpretation of the Solubility Product of UO2(S)", submitted to Acta Chem. Scand. (1988)

BRUTON C., H. SHAW, "Geochemical simulation of reaction between spent fuel waste form and J-13 water at 25oC and 90oC", Mater. Res. Soc. Symp. Proc. Vol. 112, (1988) 485-494.

CONTAMIN P., J.J. BACMANN, J.F. MARIN, "Autodiffusion de l' oxygene dans le dioxide d'uranium surstochiometrique", J. Nucl. Mater. 42 (1972) 54-64

COWEN G.A., "Migration Path for Oklo Reactor Products and Applications to the Problem of Geological Storage of Radioactive Waste", in 'Natural Fission Reactors', IAEA, CONF-771222, pp. 693-699 (1978)

CRANK J., "The Mathematics of Diffusion", At The Clarendon Press, Oxford (1955)

CURTIS D.B., "The Chemical Coherence of Natural Spent Fuel at the Oklo Natural Reactors", KBS Technical Report TR-85-04 (1985)

DOREMUS, R.H. "Interdiffusion of Hydrogen and Alkali Ions", J.Non Cryst.Solids, 19, pp. 137-144 (1975)

DU PREEZ J.G.H., D.C. MORRIS, C.P.J. VAN VUUREN, "The chemistry of uranium. Part XXVII. Kinetics of the dissolution of uranium dioxide powder in a solution containing sodium carbonate, sodium bicarbonate and potassium cyanide", Hydrometallurgy, 6 (1981) 197-201

EARY L.E., L.M. CATHLES, "A kinetic model of UO_2 dissolution in. acid H_2O_2 solutions that includes uranium peroxide hyfrate precipitation", Metall.Trans.B,148(1983)325.

EINZIGER R.E., R.E. WOODLEY, "Predicting spent fuel oxidation states in a tuff repository", HEDL-SA-3627, Westinghouse Hanford Company, Richland WA, USA, 1987

EINZIGER R.E., R.E. WOODLEY, "Low temperature spent fuel oxidation under tuff repository conditions", HEDL-SA-3271FP, Westinghouse Hanford Company, Richland WA, USA, 1985

EKLUND U.B., R.S. FORSYTH, KBS Technical Report No 70, Stockholm, Sweden 1978

FORSYTH R.S., L.O. WERME, "The Corrosion of Spent UO2 Fuel in Synthetic Groundwater", Mat. Res. Soc. Symp. Proc. Vol. 50, Materials Research Society, Pittsburgh, PA 15237, pp. 327-336 (1985)

FORSYTH R.S., "Fuel rod D07/B15 from Ringhals 2 PWR: Source material for corrosion/leach tests in groundwater - Fuel rod/pellet characterization program part one", SKB Technical Report 87-02, Stockholm, Sweden (1987)

FORSYTH R.S., L.O WERME, J. BRUNO, "The corrosion of spent uranium dioxide fuel in synthetic groundwater", J.Nuc.Mat.138 (1986)1

FORSYTH R.S., L.O. WERME, "Corrosion tests on spent PWR fuel in synthetic groundwater". Studsvik Report. 87/18 (1987)

FORSYTH R., K. SVANBERG K., L.O. WERME, "The corrosion of spent UO_2 fuel in synthetic groundwater", Mat. Res. Soc. Symp. Proc. 26, 1984

GARISTO N.C., GARISTO F., "The effect of precipitation on the long-term release of radionuclides from used fuel", Ann. Nucl. Energ., 13, 11, 1986

GARISTO F., "Solid dissolution effect of mass transport- precipitation coupling", Chem. Eng., Sci., 41, 12, 1986

GARISTO N.C., GARISTO F., "The dissolution of UO_2. A thermodynamic approach". Nucl. Wast. Mang.,6, (1986) 203.

GRANDSTAFF D.E., "A kinetic study of the dissolution of uraninite". Econ. Geol. 71, (1976) 1493

GRAY W., "Comparison of Uranium Release from Spent Fuel and Unirradiated UO_2 in Salt Brine", Mat. Res. Soc. Symp. Proc. Vol 84, (1987), 141-152.

HABASHI F., G.A. THURSTON, "Kinetics and mechanisms of the dissolution of uranium dioxide", Energ. Nucl. 14 (1967) 238

HASTINGS I.J. et al., "Postirradiation Behavior of UO_2 Fuel II: Fragments at 175 to 275°C in Air", Nuclear Technology 68 (1985) 40-47

HAWKINS R.J., C.B. ALCOCK, J. Nucl. Mater. 26 (1968) 112/22

HISKEY J.B., "Kinetics of uranium dioxide dissolution in ammonium carbonate", Trans. Inst. Min. Metall. Sect. C, 88 (1979) C145

HISKEY J.B., "Hydrogenperoxide leaching of uranium in carbonatye solutions", Trans.

Inst. Min. Metall. Sect. C, 89 (1980) C145

HOEKSTRA H.R., A. SANTORO, S. SIEGEL, "The Low Temperature Oxidation of UO_2 and U_4O_9", J. Inorg. Nucl. Chem., 18 166-178, 1961

JOHNSON L H., et al., "Mechanisms of leaching and dissolution of UO_2 fuel", Nucl. Techn. 56 (1982)

JOHNSON L.H., SHOESMITH D., "Spent fuel", in 'Radioacitve Waste Forms for the Future' eds. W. Lutze, R. Ewing, Elsevier Science Publ., New York (1988)

KUZ'MICHEVA E.U., L.M. KOVBA, E.A. IPPOLITOVA, "Oxidation of Uranium Dioxide at Temperatures Below 270°C", Sov. Radiochem. 13 (1971) 877-881

LAY K.W., J. Amer. Ceram. Soc. 52 (1970) 369-73

MATZKE H., Diffusion in Ceramic Oxide Systems, in 'Fission-Product Behavior in Ceramic Oxide Fuel', ed. I.J. Hastings, Advances in Ceramics Vol. 17, 1986, pp.1 - 54, American Ceramic Society, Columbus, Ohio, USA

MATZKE H., "Atomic transport properties in UO_2 and mixed oxides (U,Pu)O2", J. Chem. Soc. Faraday. Trans 2, 1987, 83

McINTYRE N.S., S. SUNDER , D. SHOESMITH, "Chemical information from XPS. Applications to the analysis of electrode surfaces". J. Vac. Sci. Techn. 18, 3, 1981.

MURCH G.E., D.H. BRADHURST AND H.J. DE BRUIN, "Oxygen Self-diffusion in Non-stoichiometric Uranium Dioxide", Phil. Mag. 32 (1975) 1141-1150

NICOL M.J., C.R.S. NEEDES, "The anodic dissolution of uranium dioxide I.In perchlorate solutions", Electrochim. Acta 20 (1975) 585

NICOL M.J., C.R.S. NEEDES, "The anodic dissolution of uranium dioxide II.In carbonate solutions", Electrochim. Acta 22 (1977) 1381.

OLANDER, D.R., "Combined Grain-boundary and Lattice Diffusion in Fine-Grained Ceramics", in 'Fission-Product Behavior in Ceramic Oxide Fuel', ed. I.J. Hastings, Advances in Ceramics Vol. 17, (1986), pp. 271 - 93, American Ceramic Society, Columbus, Ohio, USA

OLLILA K., "Dissolution experiments of unirradiated uranium dioxide pellets." Nuclear Waste Commission of Finish Power Companies. Report YJT-85-02, 1985

OLLILA K., "Dissolution of unirradiated uranium oxide pellets at various parametric conditions", Nuclear Waste Commision of Finish Power Companies. Report YJT-86-28, 1986

OLLILA K., "Dissolution Mechanism of UO_2 at Various Parametric Conditions", Nuclear Waste Commision of Finish Power Companies. Report YJT-88-04, 1988

PARKHURST D.L., D.C. THORSTENSON, L.N. PLUMMER, "PHREEQE - A Computer Program for Geochemical Calculations", U.S. Geological Survey, Water-Resources Investigations 80-96, 1980, 1985

PEARSON R.L., M.E. WADSWORTH, "A Kinetic Study of the Dissolution of UO_2 In Carbonate Solution", Transaction of the Metallurgical Society of AIME, (1958) pp. 294-300

POSEY-DOWTY J, E. AXTMANN, D. CRERAR, M.BORCSIK, A. RONK, W. WOODS, "Dissolution Rate of Uraninite and Uranium Roll-Front Ores", Economic Geology, 82, 184-194, 1987

POURBAIX M., "Atlas of Electrochemical Equilibria in Aqueous Solutions", Pergamon Press, Oxford

REIMUS P.W., S.A. SIMONSON, "Radionuclide Release from Spent Fuel Under Geologic Disposal Conditions: An Overview of Experimental and Theoretical Work Through 1985", PNL-5551, Battelle Pacific Northwest Laboratory, Richland, WA 99352, USA, 1988

SCHORTMAN W.E., M.A. DE SEA, "Kinetics of the dissolution of uranium dioxide in carbonate-bicarbonate solutions." Proc.2nd Intern. United Nations Conf. Peaceful Uses of Atomic Energy; United Nations, Geneva. Vol.3., (1958) 333-341

SHOESMITH D.W., S. Sunder, B.M. IKEDA, F. KING, "The Development of a Mechanistic Basis for Modelling Fuel Dissolution and Container Failures Under Wase Vault Conditions", presented at the 12th Intl. Symp. on the Scientific Basis for Nuclear Waste Management, Berlin 1988a

SHOESMITH D.W., S. SUNDER, Anodic oxidation of UO_2.Part.III.Electrochemical studies in carbonate solutions. Pass.Metal. Semicond.ed.M.Froment.,125. 1983

SHOESMITH D.W., S. SUNDER, M.G. BAILEY, G.J. WALLACE, F.W. STANCHELL, "Anodic oxidation of UO_2. Part.IV. X-Ray photoelectron spectroscopy and electrochemical studies of film growth in carbonate-containing solutions" Application of Surface Science 20 (1984) 39-57

SIMPSON K.A., P. WOOD, "Uranium Dioxide Oxidation in Air below 350°C", US NRC Workshop on 'Spent Fuel/ Cladding Reaction During Dry Storage', held Aug. 1983, Gaithersburg, Mg. USA. NUREG/CP.0049

SMITH T., "Kinetics and Mechanism of the Oxidation of Uranium Dioxide and Uranium Dioxide Plus Fissia Sintered Pellets", NAA-SR-4677, 1960

STROES-GASCOYNE, S., et al., "Dissolution of Used Candu Fuel at various Temperatures and Redox Conditions", Mat. Res. Soc. Symp. Proc. Vol. 50, pp. 317-326, Materials Research Society, Pittsburgh, PA, USA, 1985

SUNDER S., et al., "Anodic oxidation of UO_2. Part.I. Electrochemical and X-Ray photoelectron spectroscopic studies in neutral solutions", J.Electroanal.Chem.130(1981)163.

SUNDER S., et al., "Anodic oxidation of UO_2. Part.II .Electrochemical and X-Ray photoelectron spectroscopic studies in alkaline solutions", J. Electroanal. Chem.150(1983)217.

TEMPEST P., P. TUCKER, J. TYLER, Oxidation of UO_2 fuel pellets in air at 503 and 543 K Studied using X-ray Photoelectron Spectroscopy and X-ray Diffraction, J. Nucl. Mater. 151, 1988

THOMAS G.F.,TILL G. The dissolution of unirradiated UO_2 fuel pellets under simulated disposal conditions. Nucl.Chem.Waste Manag.5,(1984)141.

THOMAS L.E., ET AL., Transmission electron microscopy of oxidized UO_2 spent fuel. Proc. 44th. Annual Meet., Elec. Micro. Soc. Amer. 1986

TAYLOR P., E.A. BURGESS, D.G. OWEN, "An X-Ray Diffraction Study of the Formation of β-$UO_{2.33}$ on UO_2 Pellet Surfaces in Air at 229 to 275°C", J. Nucl. Mater. 88 (1980) 153-160

VOLLATH D., Transport Phenomena, Gmelin Handbook, U Suppl. Vol. C5, 1986

WADSTEN T., "The Oxidation of Polychristalline Uranium Dioxide in Air at Room Temperature", J. Nucl. Mater. 64 (1977) 315

WALKER D.E.Y., "The Oxidation of Uranium Dioxides", J. appl. Chem., 128-135 (1965)

WANG R., Y.B. KATAYAMA, "Dissolution mechanisms for UO_2 and spent fuel" Nucl.Chem.Waste Manag.3(1982)83.

WANG R., "Spent-fuel Special-Studies Progress Report: Probable Mechanism for Oxidation and Dissolution of Single-Crystal UO_2 Surfaces", PNL-3566, Battelle Pacific Northwest Laboratories, Richland, WA 99352, USA, 1981

WILSON C.N., "Microstructural characteristics of PWR spent fuel relative to its leaching behaviour", HEDL-SA-3313, Westinghouse Hanford Company, Richland WA 99352, 1985

WILSON C.N., H.F. SHAW, Experimental study of the dissolution spent fuel at 85 C in natural ground water. Lawrence Livermore Nat.Lab.December 1986.

WOLLERY T.J., EQ3NR, A Computer Program for Geochemical Aqueous Speciation-Solubility Calculations: User's Guide and Documentation, UCRL-53414, Lawrence Livermore Laboratory, Livermore, California 94550, 1983

WOODLEY R.E., R.E. EINZIGER, H.C. BUCHANAN, "Measurement of the Oxidation of Spent fuel Between 140 and 225°C by Thermogravimetric Analysis", Westinghouse Hanford Company, WHC-EP-0107, 1988

YAJIMA J, H. FURUYA, T. HIRAI, J. Nucl. Mater., 20 (1966) 162-170

List of SKB reports

Annual Reports

1977–78
TR 121
KBS Technical Reports 1 – 120.
Summaries. Stockholm, May 1979.

1979
TR 79–28
The KBS Annual Report 1979.
KBS Technical Reports 79-01 – 79-27.
Summaries. Stockholm, March 1980.

1980
TR 80–26
The KBS Annual Report 1980.
KBS Technical Reports 80-01 – 80-25.
Summaries. Stockholm, March 1981.

1981
TR 81–17
The KBS Annual Report 1981.
KBS Technical Reports 81-01 – 81-16.
Summaries. Stockholm, April 1982.

1982
TR 82–28
The KBS Annual Report 1982.
KBS Technical Reports 82-01 – 82-27.
Summaries. Stockholm, July 1983.

1983
TR 83–77
The KBS Annual Report 1983.
KBS Technical Reports 83-01 – 83-76
Summaries. Stockholm, June 1984.

1984
TR 85–01
Annual Research and Development Report 1984
Including Summaries of Technical Reports Issued during 1984. (Technical Reports 84-01– 84-19)
Stockholm June 1985.

1985
TR 85-20
Annual Research and Development Report 1985
Including Summaries of Technical Reports Issued during 1985. (Technical Reports 85-01-85-19)
Stockholm May 1986.

1986
TR 86-31
SKB Annual Report 1986
Including Summaries of Technical Reports Issued during 1986
Stockholm, May 1987

1987
TR 87-33
SKB Annual Report 1987
Including Summaries of Technical Reports Issued during 1987
Stockholm, May 1988

1988
TR 88-32
SKB Annual Report 1988
Including Summaries of Technical Reports Issued during 1988
Stockholm, May 1989

Technical Reports

1989
TR 89-01
Near-distance seismological monitoring of the Lansjärv neotectonic fault region Part II: 1988
Rutger Wahlström, Sven-Olof Linder, Conny Holmqvist, Hans-Edy Mårtensson
Seismological Department, Uppsala University, Uppsala
January 1989

TR 89-02
Description of background data in SKB database GEOTAB
Ebbe Eriksson, Stefan Sehlstedt
SGAB, Luleå
February 1989

TR 89-03
Characterization of the morphology, basement rock and tectonics in Sweden
Kennert Röshoff
August 1988

TR 89-04
SKB WP-Cave Project
Radionuclide release from the near-field in a WP-Cave repository
Maria Lindgren, Kristina Skagius
Kemakta Consultants Co, Stockholm
April 1989

TR 89-05
SKB WP-Cave Project
Transport of escaping radionuclides from the WP-Cave repository to the biosphere
Luis Moreno, Sue Arve, Ivars Neretnieks
Royal Institute of Technology, Stockholm
April 1989

TR 89-06
SKB WP-Cave Project
Individual radiation doses from nuclides contained in a WP-Cave repository for spend fuel
Sture Nordlinder, Ulla Bergström
Studsvik Nuclear, Studsvik
April 1989

TR 89-07
SKB WP-Cave Project
Some Notes on Technical Issues

TR 89-08
SKB WP-Cave Project
Thermally incuded convective motion in groundwater in the near field of the WP-Cave after filling and closure
Polydynamics Limited, Zürich
April 1989

TR 89-09
An evaluation of tracer tests performed at Studsvik
Luis Moreno[1], Ivars Neretnieks[1], Ove Landström[2]
[1] The Royal Institute of Technology, Department of Chemical Engineering, Stockholm
[2] Studsvik Nuclear, Nyköping
March 1989

TR 89-10
Copper produced from powder by HIP to encapsulate nuclear fuel elements
Lars B Ekbom, Sven Bogegård
Swedish National Defence Research Establishment
Materials department, Stockholm
February 1989

TR 89-11
Prediction of hydraulic conductivity and conductive fracture frequency by multivariate analysis of data from the Klipperås study site
Jan-Erik Andersson[1], Lennart Lindqvist[2]
[1] Swedish Geological Co, Uppsala
[2] EMX-system AB, Luleå
February 1988

TR 89-12
Hydraulic interference tests and tracer tests within the Brändan area, Finnsjön study site The Fracture Zone Project – Phase 3
Jan-Erik Andersson, Lennart Ekman, Erik Gustafsson, Rune Nordqvist, Sven Tirén
Swedish Geological Co, Division of Engineering Geology
June 1988